School of Graduate Studies

Green Synthesis and Characterization of Magnetite (Fe_3O_4) nanoparticle using Khat *(Catha edulis*) plant leaf extract for the removal of methylene blue dye from aqueous solution

Metaalem Shibabaw

A Thesis submitted to Department of Chemistry College of Natural and Computational Science in the Partial Fulfillment of the Requirements for the Degree of Master of Science in Chemistry

January, 2025

Wolkite, Ethiopia

Wolkite University

School of Graduate Studies

Green Synthesis and Characterization of Magnetite (Fe_3O_4) nanoparticle using Khat *(Catha edulis*) plant leaf extract for the removal of methylene blue dye from aqueous solution

A Thesis submitted to Graduate Studies in the Partial Fulfillment of the Requirements for the Degree of Master of Science in Chemistry

Metaalem Shibabaw

Major Advisor: Nigussie Alebachew (PhD)

Co-advisor: Israel Leka (PhD)

January, 2025

Wolkite, Ethiopia

DECLARATION

I declare that this thesis study entitled **"Green Synthesis and Characterization of Magnetite (Fe_3O_4) nanoparticle using Khat *(Catha edulis*) plant leaf extract for the removal of methylene blue dye from aqueous solution,"** in partial fulfillment of the requirements for the degree of Master of Science in applied Chemistry is my own work and has not been submitted to any university for similar purpose. The references used in this thesis study are duly recognized by proper citations.

Name of student	Signature	Date
_____	_____	_____

RECOMMENDATION

We, the major advisor and co-advisor of this research study, hereby certify that we have closely advised the student while developing this research and read the draft thesis study entitled **"Green Synthesis and Characterization of Magnetite (Fe_3O_4) nanoparticle using Khat *(Catha edulis*) plant leaf extract for the removal of methylene blue dye from aqueous solution,"** prepared under my guidance by **Metaalem Shibabaw**. Therefore, we recommended the submission of the thesis research to the department for further review and evaluation.

_____	_____	_____
Advisor	Signature	Date
_____	_____	_____
Co-advisor	Signature	Date

APPROVAL SHEET

We, the major advisor and co-advisor of the thesis entitled **"Green Synthesis and Characterization of Magnetite (Fe_3O_4) nanoparticle using Khat *(Catha edulis*) plant leaf extract for the removal of methylene blue dye from aqueous solution,"** and developed by **Metaalem Shibabaw**, hereby certify that the recommendation and suggestions made by the board of examiners are appropriately incorporated in to the final version of the thesis

_____ _____ _____

Major Advisor Signature Date

_____ _____ _____

Co-advisor Signature Date

We, the members of the Board of Examiners of the thesis by **Metaalem Shibabaw** have read and evaluated the thesis entitled **"Green Synthesis and Characterization of Magnetite (Fe_3O_4) nanoparticle using Khat *(Catha edulis*) plant leaf extract for the removal of methylene blue dye from aqueous solution,"** examined the candidate during the open defense. The thesis is accepted for partial fulfillment of Master of Science in Chemistry.

1._____ _____ _____

Name of External Examiner Signature Date

2._____ _____ _____

Name of Internal Examiner Signature Date

3._____ _____ _____

Name of Chairman Signature Date

Final approval and acceptance of the thesis are contingent upon the submission of its final copy to the Office of Postgraduate Studies (OPGS) through the Department Graduate Council (DGC) and School Graduate Committee (SGC).

_____ _____ _____

Department Head Signature Date

_____ _____ _____

School of graduate studies Signature Date

_____ _____ _____

Office of Postgraduate coordinator Signature Date

ACKNOWLEDGEMENT

First and foremost, I would like to thank the Almighty God and his mother St. Marry for giving me the health, strength, wisdom, and patience to complete this thesis.

Second, I would like to express my deepest gratitude and thanks to my advisor Nigussie Alebachew (PhD) for his cooperation, suggestions, supervision and remarks, appreciable encouragement, fatherly consultation, and taking his time to read and correct my document, starting from the proposal writing to the completion of this thesis.

I would like to thank my co-advisor Dr. Israel Leka, my colleagues, Chemistry Laboratory Technicians, Applied Chemistry Department, Dr. Megersa Feyissa, and all individuals who supported me by sharing ideas or offering material support which is an input for this work.

I would like to transfer also my special thanks to Wolkite University, Chemistry Department, for synthesis of magnetite nanoparticle experiment, and Addis Ababa Sciences and Technology University, Central Laboratory and Adama Sciences and Technology University for FT-IR, XRD, SEM and UV-DRS analysis.

Contents Pages

LIST OF TABLES

LIST OF FIGURES

Figure description **Page**

LIST OF ABBREVIATIONS

AAS	Atomic absorption spectroscopy
DMSO	Dimethyl sulfoxide
DNA	Deoxyribose nucleic acid
EDX	Electronic diffraction X-ray
EPA	Environmental Protection Agency
FTIR	Fourier transforms infrared spectroscopy
MRI	magnetic resonance imaging
Nm	Nanometer
NPs	Nanoparticles
PHpzc	PH at point of zero charge
RSM	Response Surface Methodology
SEM	Scanning electron microscopy
TGA	Thermal gravimetric analysis
UV-Vis	Ultraviolet- Visible spectroscopy
XRD	X-ray diffraction

ABSTRACT

This study synthesized magnetite nanoparticles using an aqueous extract of Catha edulis leaf in a green manner. The effectiveness and ability of the resultant nanoparticles in removing Methylene Blue dye were also assessed. Utilizing SEM, FTIR, P-XRD, and UV-DRS spectroscopy, the produced nanoparticle was examined. According to the XRD data, the average particle size of the produced magnetite NPs was 9.05 nm. The outcome confirmed that Fe_3O_4 nanoparticles had absorbance maxima at 364 nm, and for samples of produced magnetite nanoparticles, various functional groups were discovered to be connected with the plant extract. The produced Fe_3O_4 NPs displayed a variety of morphologies and microstructural features for Fe_3O_4 nanopowder. In addition, the SEM images of the Fe_3O_4 NPs showed that the nanoparticle morphology was uniform in structure. Using the batch adsorption method, the effectiveness of the adsorbent was assessed by adjusting several parameters, including pH (3–9), adsorbent dose (20–80 mg), initial adsorbate concentration (5 mg/L–20 mg/L), and room temperature contact time (30–90 minute). Optimal removal (99.25%) was achieved at pH 9, using 20 mg of adsorbent, 50-minute contact time, and an initial methylene blue concentration of 5 mg/L. The Langmuir isotherm model and pseudo-second-order kinetics model best described the experimental data ($R^2 \approx 1$). This research suggests that the biosynthesized Fe_3O_4 nanoparticles show significant potential in the removal of methylene blue dye from aqueous solutions.

Keywords: Magnetite NPs, Green synthesis, Waste water, isotherm model, kinetics model.

CHAPTER ONE

1. INTRODUCTION

1.1 Background of the study

Nanotechnology is becoming an emerging multidiscipline field of science attracts scholars' attention is playing a significant role in many fields such as in energy, environment, medicine and others. This is due to so many reasons like their large specific surface area, specific Uv-Vis range of light absorption and extremely small size (in nanometers), which results modifications in the properties of compounds. Nanoparticles are also used for environmental remediation processes such as elimination of organic toxins like dyes and detection of heavy metals and pollutants [1]. Globalization and rapid urbanizations have led to the prosperity of human life but also to the environmental pollution and biological destruction of the world. All environmental matrices are constantly at risk of contamination by organic and inorganic pollutants [2].

Previous studies show that water which is released from various industries contains various pollutants and synthetic dyes are one of the most important pollutants in waste water. Removing organic dyes from such sources is still at the early stage because of degradability, carcinogenicity and mutagenicity of dyes [3].Various techniques are used to remove these pollutants from wastewater. Adsorption is considered the most popular, effective and economic method to remove various pollutants from water [4]. In recent years, water scarcity and pollution problems have reached serious levels worldwide. Currently, approximately 3.1% of annual deaths worldwide (i.e. more than 1.7 million people) are due to a lack of reliable drinking water sources [5]. The main cause of drinking water scarcity is pollution. In all developing countries, efforts should be made to prevent water pollution from organic contaminants such as methylene blue, rhodamine, methyl red, malachite green, and metals such as cobalt, copper, nickel, lead, zinc, and chromium [6].

Organic pollutants such as dyes are one of the major pollutants generated by various industries, especially the chemical industry, textile industry, dye manufacturing, pigment and dyeing industries, etc. These pollutants which are released in to the atmosphere causes critical risks among the human's organic body like the kidneys, central nervous system, reproductive system,

heart and brain. This situation creates an urgent need to science and technology to quickly and effectively remove pollution and waste from the marine environment. There are many physical, chemical and biological treatment approaches accessible to eliminate organic chemicals, heavy metals and harmful organisms from wastewater. The adsorption process is one of the physical methods applied to remove organic and inorganic pollutants released from different sources [7]. Among widely used adsorbents, biosynthesized nanoparticles are the most popular because they are synthetic, non-toxic, environmentally friendly, and inexpensive with high adsorption capacity. Metal oxide nanoparticles have become popular among scientists due to their medical applications, MRI [8], and adsorption of environmental impurities [9].

One of the most important metal oxide nanoparticles is magnetite; that has unique properties that can be used for various heaths, environmental, medicinal and therapeutic purposes [10]. Here, khat leaf extract was used as a reductant and capping agent for production of magnetite nanoparticles. Khat leaf extract contains alkaloids, cathine dimer and cathinones, triterpenes, sterols, fatty alcohol, hydrocarbon carboxylic acid and saponin. The alkaloid, cathinone, may be the chief psychoactive component of khat. In addition, the leaf extract was chosen because it is available in the environment and contains chemicals that reduce and fix active ingredients. Studies have shown that biomolecules such as polyphenols, saponins, organic acids, vitamins, polysaccharides and terpenoids play a role in the reduction and capping of nanoparticles. Currently, the environmental nanoparticle synthesis processes is designed to be non-toxic during production. Therefore researchers in the field of nanoparticle production and assembly have turned their attention to natural processes [11].

In the last 20 years, the synthesis of nanoparticles from plant extracts has attracted much attention. This is probably due to their simple, rapid, non-toxic and effective reaction [64]. In this study, a green process was developed for the preparation of iron oxide nanoparticles (Fe_3O_4 NP) from khat leaf extract. The method is convenient and simple, providing potential for the production of nanoparticles. Khat is a fast-growing plant used mainly as a stimulant in Yemen and African countries such as Ethiopia and its leaves contain many phytochemicals. These substances are extracted from Khat and used as a reducing agent and surfactant in the reaction. The structure and morphology of magnetite nanoparticles were confirmed using multidisciplinary characterization tools.

The synthesized magnetite nanoparticle was selected as highly efficient nano-adsorbent due to its small size, high permeability, large specific surface area, high reactivity, catalytic efficiency and super paramagnetic properties. The NP has unique catalytic activity due to its small size, large specific surface area and high degree of dispersion. The chemical and surface properties of the nanoparticles were characterized and found be promising adsorbents in the removal of aqueous methylene blue dye. The pH of the solution, time, adsorbent amount and initial concentration of MB dye were studied and the equilibrium kinetics and adsorption parameters were evaluated. The behavior and mechanism of adsorption were also studied [11].

1.2 Statement of the problem

The world is currently facing increasing water pollution from effluents from various industries. Among them, dyes released from the textile industry are the main pollutants. The yearly global fabrication of dyes is around 7×10^5 tons, and about 10-15 percent of dyes utilized are discharged into water. Artificial dyes are more challenging to eliminate than natural dyes due to their complicated aromatic arrangement that provides stability in air and light. They can be simply transported into aquatic surroundings due to high solvability in water. They influence marine autotrophy through limiting the photosynthesis effectiveness, since merely a partial amount of light is permitted to enter due to their color; its poisonous influence spreads along the food chain and stored for long times, worsening the health of animals and humans [12].

Some fundamental problems motivated for the green production of magnetite nanoparticles (Fe_3O_4) with Catha edulis plant leaf extract for the elimination of methylene blue from wastewater. The first is that due to population growth and industrial development, environmental pollution is increasing due to the lack of water treatment. For this reason, practical and inexpensive methods, including adsorption, have attracted a lot of attention in recent years. In this research study, magnetite nanoparticles were prepared from iron oxide by applying a bioactive compound present in the leaf extract of the khat plant as it is a green synthesis, safe for the environment, non-toxic, cost-effective and synthesized using locally available sources such as khat (Catha edulis).

Several approaches have been advanced in combination with nanoparticles that provide nanotechnology for the elimination of dyes like rhodamine and MB from wastewater. Adsorption is the furthermost widely utilized method for the elimination of dyes from contaminated water

because it is cheap, easy to use as well as lack of formation of subordinate pollutants. Thus, in the current investigation, a magnetite nanoparticle that was produced through green extraction of khat leaf extract was selected as nano-adsorbents that showed higher efficiency and faster adsorption rate thanks to its small size, high permeability, large vigorous superficial area, high reactivity, catalytic efficiency and superparamagnetic properties.

1.3 Objective of the study

1.3.1 General objective of the study

The general objective of this study was to synthesize and characterize magnetic magnetite nanoparticles using khat (*Catha edulis*) for the elimination of methylene blue from an aqueous solution.

1.3.2 Specific objective of the study

- ✓ To characterize the synthesized magnetite nanoparticles using khat plant leaf extract.
- ✓ To study the efficiency of methylene blue dye removing from aqueous solution using the synthesized nanoparticles.
- ✓ To assess the consequence of pH, time, adsorbent quantity and initial concentration parameters on the adsorption efficiency of nanoparticles.
- ✓ To describe the adsorption process using sorption isotherm & sorption kinetic model.

1.4 Significance of the proposed study

The major advantage of this study is that the desired materials are separated from the solution in a simple and compact process. Another advantage is due to the fact that magnetite nanoparticles will be synthesized by a green process from Catha edulis leaf extract, the method is environmentally friendly. The study uses a low-cost, locally available plant leaf extract, khat (Catha edulis). The use of magnetite nanoparticles as an adsorbent in wastewater treatment provides a practical approach to remove contaminating dyes from water. The study provides the community with information on green synthesis and helps in the use of magnetite nanoparticles synthesized with khat (Catha edulis) as a dye bioadsorbent. The result obtained can serve as a basis for other studies on the biosynthesis of nanoparticles and their use in environmental protection.

1.5 Scope of the study

This study was limited to green synthesis and characterization of magnetite (Fe_3O_4) nanoparticles utilizing khat plant leaf extract for the elimination of methylene blue dyes from an aqueous solution and their characterization of the synthesized nanoparticles by SEM, XRD, FTIR and UV-DRS spectroscopy techniques.

CHAPTER TWO
2. LITERATURE REVIEW

2.1 Nanotechnology

Nanotechnology is essentially the manipulation of material at molecular and microscopic levels to create other structures, devices and systems with enhanced electrical, optical, magnetic and conductive properties. Nanotechnology has been evaluated as a promising technology and significant results in different areas, including wastewater management. Due to their small size, large surface area, and ease of manipulation, nanostructures offer unique opportunities for creation of simple accelerators and redox-active media in wastewater treatment. Nano-materials can remove many pollutants in wastewater, such as heavy metals, organic and inorganic solvents, dyes, and even pathogenic diseases such as cholera and typhoid [13].

Extraction of various plant sources is used as reducing agents and capping agents in the production process. Modest and environmentally friendly methods have been proposed for production of plant nanoparticles (NPs) using aqueous extract of various plants and plant-derived phenolic composites play an important role as non-toxic reducing agents and capping agents for NPs [14]. Nanoparticles and their composites are believed to have strong inhibitory and antibacterial properties against bacteria, viruses and fungi. Due to the spread of diseases caused by various pathogenic microorganisms in today's world, the developments of antibiotic, green production, behavioral patterns and utilization of nanoparticles (NPs) have become important topics in nanotechnology. Green production of nanoparticles has been developed universally and has many applications; the system is extremely safe and environmentally friendly [14].

2.2 Nanoparticles (NPs)

Nanoparticles are nanometer sized particles, between 1 nm and 100 nm, surrounded by an interface layer. The green production methods of nanoparticles have attracted attention of scientists due to their synthesis process. Almost all types of biological methods are used to produce nanoparticles in a size and shape-controlled manner [15]. Of course, nanoparticles are mostly found as biological molecules, ash, soil particles or synthetically produced for use in certain areas. Green produced metal nanoparticles are being studied by scientists due to their special properties, and therefore the biological molecules found in the plant extracts play an

important role as stabilizers and reducing agents [15]. Like the most common inorganic nanoparticles, metal and metal oxide nanoparticles also represent a group of materials and compounds evaluated for various biomedical applications.

Studies have shown that the size of the nanoparticles is important in determining the antibacterial properties of these materials. The bacterial cell wall attracts nanoparticles to its surface through electrostatic attraction. These nanoparticles form a strong bond with the membrane, increasing the permeability of the cell wall. Metal nanoparticles and metal ions, released from nanoparticles, can enter cells and cause oxidative stress, disrupting the microbial antioxidant defense response to oxygen cell functions. These ions can interact with cell structures and form strong, non-specific coordination bonds with nitrogen (N), oxygen (O) or sulfur (S) atoms found in organic dyes, ultimately disrupting biological processes in many microorganisms [16].

Scholars are tired of using new tools to create new nanoparticles that will expand many areas of use. The use of nanoparticles to improve wastewater management is an aspect of nanotechnology. There are fewer details about the recent developments in this field of research area. The use of nanomaterials in water and wastewater management is an encouraging trend and many studies report success. [17].

Iron oxide is sought after by scientists due to its many properties. Magnetite is among the most important iron oxide nanoparticle, having an inverse cubic spinel structure is used more than other magnetic nanoparticles due to its biocompatibility [18]. This structure provides special properties that can be used in various medicinal applications [19]. Magnetite nanoparticles are very popular nano-adsorbents. Their good physical and chemical properties, free concept, and easy recovery in external and attractive fields allow them to be used as materials in water treatment [20]. Magnetic nanoparticles are also useful for many applications, including biomedical applications such as antibiotics. However, the surface of the nanoparticles must be functional. For magnetic nanoparticles to be biocompatible, they must have superparamagnetic behavior and high saturation magnetization [21].

2.2.1 Synthesis of nanoparticles

Different methods for syntheses of nanoparticles have been proposed generally top-down (physical methods), bottom-up (chemical methods) and green (biological methods). Chemical or physical methods are generally used in the preparation of metal nanoparticles. However, the

chemicals used in physicochemical methods are usually expensive, harmful and flammable, while biological methods are efficient, cost-effective, energy-saving and environmentally friendly by the synthesis of iron oxide (magnetite) nanoparticles by various microorganisms and plants. This biosynthetic method is quite simple and requires less time and effort than physical and chemical methods. Another competitive advantage is that biological methods are the availability of biological resources, the time required is short, and the prepared nanoparticles can be dissolved in water [22].

2.2.2 Synthesis of magnetite nanoparticles

There are several physicochemical methods for the synthesis of magnetite nanoparticles. Most of these methods divided into two types: polymer or surfactant-supported precipitants and co-precipitation reactions. The Production methods include micro-emulsion, polyol, sonolysis, co-precipitation, gas aerosol, sol-gel, electrochemical decomposition, and the green synthesis methods (other nanoparticle synthesis method).

Table 1: Different chemical techniques for the production of magnetite nanoparticles

Method	Synthesis details	Advantage	References
Micro emulsion	Iron salt and alkali solution mixing and dispersion penetration into the oil phase integrates surfactants.	Variety of magnetite nanoparticles are processed by changing the nature, surfactant concentration and conditions of a reaction.	[23, 24, 25]
Polyols	The Iron salt is dissolved in the polyol solvent. The suspension is whisked and boiled. Polyols act as reducing and stabilizer.	Direct of particle amplification is a version of inter particle accumulation and obtain clear shapes of particles.	[26, 27, 28]
Sonolysis	Ultrasonic separation of organometallic precursors.	Achieved high magnetization and crystallinity.	[29, 30, 31]
co-precipitation	The process involves alkalization of iron and iron species.	allow for uniform nanoparticle sizing	[32]
gas aerosol	Many iron salts and a reducing agent in organic	Different sizes and shapes of particles are enclosed by	[33, 34, 35]

	solvent are dispersed into reactors and aerosol solutes are compressed and solvent dispersion occurs.	using different iron precursors.	
sol-gel	Hydroxylation and condensation of molecular precursors in a liquid are known as “sol,” when a solvent evaporates to encompass 3D networks of nanoparticles is called “gel.”	The size and stability of particles in sol-gel matrix must be controlled.	[36]
electrochemical decomposition	Iron oxide nanoparticles are manufactured by the oxidation of iron electrode in aqueous solution	Particle size is controlled by adjusting current density.	[37, 38, 39]
Green synthesis	Nanoparticles are produced using green stabilizers without the use of chemicals.	There is no chemical that are used as reducing agent and preservatives which are hazardous to the environment.	[40]

2.3 Waste water treatment

Wastewater contains many hazardous substances and comes from many sources including domestic sewage, commercial waste, industrial waste and agricultural waste. The main sources of wastewater are domestic water, agricultural waste, industrial waste and commercial waste. Large water bodies usually need good quality water, but on the contrary, a lot of dirty water and poor-quality water are discharged in to large water bodies, causing them to be polluted [13].

2.3.1 Nanotechnology in wastewater management

Methods based on nanotechnology in wastewater treatment include Nano filtration, photo catalysis, adsorption and bio sorption, disinfection and disease control, detection and maintenance, etc.

Adsorption is considered as the deposition of mass on a surface or interface between two phases. The tissue that accrues on the surface is called adsorbate and the place where the accumulation occurs is called adsorbent. It is classified into two as physical and chemical adsorption. There is an ionic or chemical interaction between the adsorbent and the adsorbate in chemisorption. Chemisorption is generally, a very effective process. While in physical adsorption, mass accumulation occurs due to van der Waals attraction, hydrogen bonds and interpolar interactions, etc., therefore the process is usually reversible in most cases. In addition to dye removal, the chemical adsorption methods are also widely used to remove heavy, toxic or beneficial substances, anionic groups, toxic biological chemicals, pollutants, etc. [41]. Other technologies are generally not popular due to their high operating costs and time-consuming processes. However, adsorption has proven to be a more powerful technique for the treating organic and inorganic pollutants because it is cheap, simple and insensitive to toxic substances [42].

Biosorption is a passive, independent metabolism in which dissolved substances (biosorbates) can be adsorbed from the liquid phase to the surface of the biomass (biosorbent). Biosorption is one of the effectivet sorption processes resulting from the difference in concentration of biosorbate molecules between the liquid phase and the biosorbent material. The presence of functional groups on the surface of biosorbents is essential for the physical or chemical interactions with biosorbates of the liquid mixture. Biosorption has proven to be an effective and efficient alternative to traditional water treatment technology. The abundance of biosorbents, their biodegradability, various surface functions and ease of modification have attracted many

researchers who hope to use their potential for the removal of various pollutants in batch or continuous process. However, there are fewer reports on continuous biosorption [43].

2.3.2 Magnetite (Fe_3O_4) nanoparticles for removal of MB dye

Nanomaterials have many advantages over other adsorbents; however, they can cause toxicity because of their unique structure, smaller size, and related chemical and physical features, even at low concentrations. As example, TiO_2 at the nano scale causes hemagglutination, irregular sedimentation, and hemolysis of red blood cells [44]. In addition, the widespread use of nanoparticles in applications such as cosmetics, electronics, and water treatment has led to the unintentional release of nanomaterials into the environment [45]. Therefore, nanomaterials need to be separated from water by appropriate purification. To minimize this problem, magnetite nanoparticles and their modified materials have been applied. Magnetite nanoparticles exhibit superparamagnetic behavior, i.e., they are attracted by the applied magnetic field but no longer retain magnetism after the magnet is removed. By applying an external magnetic field, superparamagnetic particles can be easily and quickly removed from the bulk water samples [46]. In addition, the reuse of the magnetic adsorbent allows the adsorbed dye molecules to be used in adsorption cycles after desorption from the surface of the magnetic adsorbent. Therefore, magnetite nanoparticles are considered as economical, effective, and abundant, easily available, magnetically separated adsorbents that can adsorb dye molecules from simple water samples [64].

2.4 Factors that affect adsorption

2.4.1 Effects of solution pH

The efficiency removing dyes increases with increasing pH of the solution until equilibrium is reached. Increasing the pH leads to the formation of surface charges on the adsorbent and also to the occurrence of deprotonating reaction. This charge allows high removal efficiency due to the electrostatic attraction between the adsorbent and the adsorbent charge, while at lower pH the different functional groups and reactive atoms of the dyes and the adsorbent are either protonated or charged. Therefore, due to the strong repulsion between the dyes and the adsorbent, the removal percentage decreases [48].

2.4.2 Effects of adsorbent dose

Increasing the amount adsorbent will lead to an increase in specific surface area; therefore, more active sites are available to bind the dye from an aqueous phase. If the adsorption dosage is reduced, the amount of MB dye adsorbed decreases, due to the accumulation and covering of adsorbent particles in the solution, a decrease in surface area for MB dye adsorption occurs [48].

2.4.3 Effects of initial concentration

The ability of the adsorbent increases as increasing dye concentration until saturation is reached. The initial dye concentration generates a large driving force to overcome the resistance to dye mass transfer between the solid and aqueous phases. The adsorption rate increases with increasing adsorbate concentration [48].

2.4.4 Effect of contact time

The concentration of adsorbed dyes in wastewater increases with time. The adsorption of toxic dyes was examined at different time intervals (0 to 50 minute). The results showed that adsorption equilibrium was reached after only 50 minutes [48].

2.5 Kinetics studies

The kinetic curves provide information on the rate of absorption and also the time required to reach equilibrium. The dye absorption data fit well with pseudo-2nd-order kinetics, giving linear plots with high correlation coefficients (R^2). In addition, the experimental values of qe (mg/g) are in excellent agreement with the values of qe (mg/g) calculated from the pseudo-2nd -order model. Combined with the poor fit to first-order kinetics, the sorption is considered a pseudo-2nd -order kinetics. Thus, chemisorption and the rate depend on the number of magnetite surface sites [20].

Pseudo-second order kinetics equation

$$\frac{t}{qt} = \frac{1}{k_2 qe^2} + \frac{t}{qe} \quad \text{..... Eq(1)}$$

Where qe (mg/g) is amount of MB uptake at equilibrium time; qt (mg/g) is the amount of MB uptake at a time, t (min); K_2 is the pseudo 2nd-order rate constant. The kinetic rate constant, k, and qe for each model can be determined by plotting graph log t/qt versus t for pseudo-2nd order models.

2.6 Equilibrium isotherm studies

Adsorption isotherms pronounce how the adsorbate interacts with the adsorbent and providing detailed insight into the nature of the interaction. An isotherm also helps in providing information on the optimal use of adsorbents. Isothermal curves are very important in adsorption purposes, as they provide information on the interaction mechanisms and the maximum adsorption capacity of a given adsorbent [47]. To develop the most appropriate biosorption isotherm model, equilibrium data were analyzed using the most common isotherm models, such as the Langmuir and Freundlich isotherm models. They were useful in determining the maximum adsorbate adsorption capacity for a given adsorbent. They differ in the basic hypothesis, the shape of the isotherm and the nature of the adsorbent surface. The Freundlich isotherm is derived by assuming a heterogeneous surface with a non-uniform distribution of the heat of adsorption on the surface. While in the Langmuir theory, the basic assumption is that sorption occurs at specific homogeneous sites in the adsorbent [47].

The mathematical expressions for those isotherms were presented in the equation:

$$\frac{C_e}{qe} = \frac{1}{bq_m} + \frac{C_e}{q_m} \quad \text{.....Eq (2)}$$

$$logq_{e=logK_f} + \frac{logC_e}{n} \quad \text{.....Eq (3)}$$

Where Ce is the equilibrium concentration of solute (mmol L^{-1}), qe is the amount of solute adsorbed per unit mass of adsorbent (mmol g^{-1} of adsorbate), qm is the adsorption capacity (mmol g^{-1}), or monolayer capacity, and b is a constant (L $mmol^{-1}$) for Langmuir isotherm, Kf and n are empirical constants for Freundlich isotherm incorporating all parameters affecting the adsorption process such as, sorption capacity and sorption intensity respectively. The isotherm curves are plotted Ce/qe versus Ce for Langmuir isotherm and log qe vs log Ce graph for the Freundlich isotherm model [47].

CHAPTER THREE

3. MATERIALS AND METHODS

3.1 Study sites description

The green production of magnetite (Fe_3O_4) nanoparticles using Catha edulis leaf extract and their characterization and evaluation of the removal efficiency of methylene blue dye from aqueous solution were carried out in the laboratory of the chemistry department of Wolkite University. However, some of the characterizations were carried out in different places due to the lack of some instruments. SEM, XRD, FTIR and Uv-DRS characterizations were carried out in Adama and Addis Ababa universities.

3.2 Chemicals and instruments

3.2.1 Chemicals and samples

The chemicals used during this research work were of analytical grade such as iron (II) chloride tetrahydrate ($FeCl_2.4H_2O$) (Sigma aldrin, 99% purity), iron (III) chloride hexahydrate ($FeCl_3.6H_2O$), (Sigma aldrin, 99% purity), distilled and tap water (H_2O), ethanol (C_2H_5OH 99.8%) (Fmd, Ethiopia) and sodium hydroxide (NaOH), (Sigma aldria 99% purity), HCl (Riedel dehaen Germany, 37%), H_2SO_4 (Sigma aldrin, 98% purity) and khat leaves (Catha edulis). Every aqueous solution is prepared with refined water.

3.2.2 Apparatus and instruments

The equipment and tools used included: a pipette, an electrical balance, a beaker, a magnetic stirrer with a hot plate, a Petri dish, a conical flask, flasks, funnels, a graduated cylinder, filter paper for filtering the extract. , a crucible, a mortar and pestle, a dropper, a centrifuge and sample characterization instruments included; diffuse reflectance spectroscopy (DRS Elico SL-150 Uv-Vis spectrophotometer), X-Ray Diffracometer, Fourier Transform Infrared spectroscopy and Scanning Electron Microscopy.

3.3 Methods and procedures

3.3.1 Collection of Catha edulis (Khat) plant leaf

Leaves of the khat plant were bought from the local market in Wolkite, Central Ethiopia region. To remove unnecessary materials, the leaf samples were carefully washed many times with tap

water and then with purified water. To take out all traces of moisture, the cleaned khat leaves were carefully dried for about two weeks (15 days) at room temperature, in the open air and in the shade. An electric grinder was used to crush the dried leaves of the Catha edulis plant into a fine powder. The powdered and dried material was placed in storage waiting further processing.

Figure 1, Process involved in the collection of *Catha edulis* plant leaf

3.3.2 Preparation of plant leaf extract

9.0 g of powdered plant leaves were mixed with 300 mL of distilled water in a 500 mL round bottom flask for a synthesis procedure. The two components were allowed to boil at 60°C for about two hours in a round bottom flask placed on a hot plate. After allowing the boiled suspension in solution to cool for about fifteen minutes, Whatmanands #1 filter paper was used twice to filter the mixture to obtain the target leaf extract solution and stockpiled in a refrigerator at 4°C for later use.

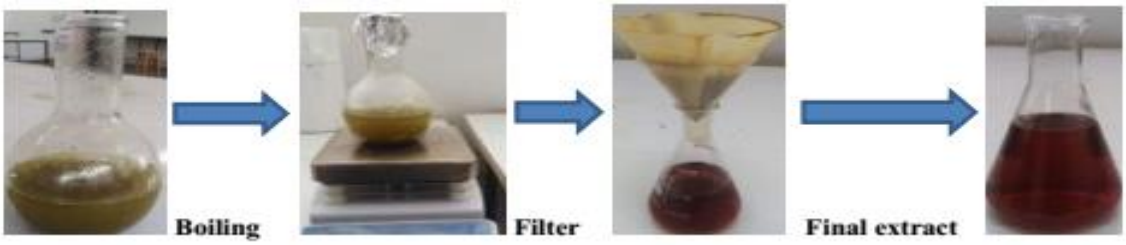

Figure 2: Process involved in the preparation of *khat* plant leaf extract

3.4 Preliminary phytochemicals tests of catha edulis leaf extract

The presence of phenols, saponins, steroids, alkaloids, glycosides, tannins (gelatin) and flavonoids in the leaf extract of the plant Catha edulis was examined according to the reported procedure [50].

3.4.1 Test for alkaloids

2 mL of H_2SO_4 and 1.2 g of iodine were mixed and diluted to a 100 mL solution. To acidify 10 mL of the extract, 1.5% (v/v) HCl was added, followed by the addition of a few drops of Wagner's reagent forms a yellow precipitate to confirm the presence of alkaloids.

3.4.2 Test for glycosides

An aqueous solution of NaOH was also mixed in one millilitre of distilled water and a small amount of the extract that had been dissolved in the latter was added. The formation of reddish brown colour indicates the presence of glycosides.

3.4.3 Test for flavonoids

2 mL of 10% (w/v) $FeCl_3$ solution and 0.5 mL of extract are mixed. On further stirred, formation of a woolly brown precipitate indicates the presence of flavonoids.

3.4.4 Test for phenols

The prepared Khat extract was treated with 3-4 drops of $FeCl_3$ solution. The product formed a bluish black colour indicating the presence of phenols.

3.4.5 Test for saponins

0.2 mL of extract was mixed with 2.0 mL of distilled water, stirred for 20 minutes leads to formation of stable foam indicates the presence of saponins.

3.4.6 Test for steroids

Two ml of extract, one ml of chloroform, and one ml of pure H_2SO_4 were carefully added to the walls of the test tube. When the garment was inspected, the chloroform stain showed a red tint, indicating the presence of steroids.

3.4.7 Test for tannins

One mL of plant extract is mixed with one mL of $FeCl_3$ solution; a greenish black precipitate is appeared to indicate the existence of tannins.

3.5 Synthesis of magnetite NPs using khat leaf extract

Ferric and ferric chlorides were used in 1:2 ratios respectively to create magnetite (Fe_3O_4). Specifically, 1000 mL of distilled water was used to dissolve 5.3 g of ferrous chloride tetrahydrate ($FeCl_2.4H_2O$) and 10.6 g of ferric chloride hexahydrate ($FeCl_3.6H_2O$) at 80 ^{0}C using a magnetic plate. A certain ratio of khat leaf extract was added and stirred on a hot plate after 15 minutes, the light orange color started to develop. The flavonoids and polyphenols in the leaf extracts served as stabilizing and styling agents. After 5 min, the solution changed from orange to brownish black and black precipitates of magnetite (Fe_3O_4) were formed by adding 100 mL of 1 M NaOH. Also, after stirring for 5 minutes, the solution was removed from the hot plate and allowed to cool so that the iron oxide nanoparticle precipitates could settle. The black precipitates of magnetite nanoparticles (Fe_3O_4) were washed five to eight times in a centrifugation process and the precipitates were also placed in a hot air oven for 8 hours at 80 ºC. The prepared magnetite nanoparticles were stored in a hermetically sealed jar for characterization and experimental use [49]. In a usual experimentation, the extract was added to ferrous chloride and ferric chloride precursor solution in 1:2 ratios by volume like this way. For 1:2 ratios: 33.3 mL of ferrous chloride tetra hydrate, Ferric chloride hexahydrate and 66.7 mL of khat leaf extract were added. The proposed reaction scheme was:

$$Fe^{2+} + 2Fe^{3+} + \text{extract} + 8OH^- \leftrightarrow Fe(OH)_2 + Fe(OH)_3 \rightarrow Fe_3O_4 + 4H_2O$$

3.6 Characterization of magnetite nanoparticles

The obtained (Fe_3O_4) nanoparticles were examined for their maximum absorption using a UV-Vis in 200 nm to 800 nm wavelength range; the structure and phases were also characterized by XRD (X-ray diffraction); functional group analysis was performed using FTIR and the surface morphology was examined by SEM.

Using UV-Vis DRS spectrophotometers in the Department of Chemistry, Addis Ababa University of Science and Technology, the optical characteristics and band gap energy of the

biosynthesized magnetite nanoparticles were evaluated. Absorption occurred in 200-800 nm wavelength range.

The Shimadzu XRD-700 X-ray diffractometer (XRD) at Addis Ababa University Faculty of Science Department of Chemistry was used to analyze the produced Fe_3O_4 Nps. XRD evaluates crystallinity, structure defects, and crystallite size. The XRD arrays were got using Cu Kα (λ = 1.5406 Aº) radiation with 40 KV accelerating voltage, and from 10 to 80 range of 2θ was recorded at a scan rate of 20/min. The Scherrer equation can be used to estimate a particle's crystallite size D:

$$D = \frac{k\lambda}{\beta cos\,\theta}$$

Here, D is the average diameter of the crystals, the x-ray wavelength, λ is 0.154 nm, k is the structure factor, its value is assigned to be 0.94, , θ is the Bragg angle in degrees, and β is the full-width at half-height of the prominent peaks [50].

The synthesized nanomaterials were subjected to FTIR analysis at the Department of Chemistry, Addis Ababa University. FT-IR is used to determine the functional groups of the active components responsible for the generation of Fe_3O_4 NPS. Dry powder FTIR spectra of biosynthesized Fe_3O_4 samples were recorded on a FT-IR 65 (PerkinElmer) in the range 4000-400 cm^{-1} [51].

In this study, the morphological analysis of the samples was investigated using a SEM (JCM-6000plus BENCHTOP SEM, SHIMADZU Corporation, Japan) at Adama University of Science and Technology. SEM images were taken at different areas of the sample at 15.0 KV with different resolutions from 500x to 10,000x and the instrument was operated at constant beam energy.

3.7 Sorption study of MB dye by biosynthesized Fe_3O_4 nanoparticles

3.7.1 Preparation of Working Standard solution

The adsorbate molecule in the adsorption tests carried out in this work was methylene blue (MB) powder. To prepare the MB stock solution, 1 g of MB was dissolved in 1000 mL of distilled water to obtain 1000 mg/L. Using the dilution rule, additional working standard solutions of 10, 15, 20, and 25 mg/L MB were prepared from 1000 mg/L dye standard solution [52].

3.7.2 Batch sorption experiments

Using a 250 mL conical flask, a batch adsorption study was conducted for specific parameters. By varying one of the parameters while keeping the others constant, the effects of various parameters, such as pH, adsorbent dosage, adsorbate concentration, and contact time, are examined. Adsorption isotherms and adsorption kinetics are studied to determine how these factors affect the change in removal capacity. Samples are periodically removed from the flask, shaken, and filtered with Whatman filter paper for each measurement. The study included the following ranges for experimental variables: pH values (2, 4, 6, 8, and 10), adsorbent dosage (40, 60, 80, 100, 120 mg), and initial concentrations (10, 15, 20, and 25 mg/L) and contact time (30, 50, 70, 90 and 110 minutes). The absorbance of the filtered solutions was determined using a UV-visible spectrophotometer at the maximum wavelength of 664 nm and it is possible to calculate the removal efficiency of magnetite (Fe_3O_4) nanoparticles using equation 4, [52]

$$Removal\ efficiency\ (\%) = \frac{Ci-Ce}{Ci} x\ 100 \quad \ldots\ldots\ldots\ldots\ldots\ldots\ldots\ldots\ldots\ldots \text{Eq(4)}$$

Where C_i is the initial concentration (mg/L) and Ce is the residual (equilibrium) concentration (mg/L) of the MB being studied.

The removal capacity of magnetite nanoparticle is the amount of MB adsorbed per unit mass of adsorbent will be calculated based on the principle of mass balance using Equation 5, [20].

$$Removalcapacity\ (qe) = \frac{Ci-Ce}{m} xv \quad \ldots\ldots\ldots\ldots\ldots\ldots\ldots\ldots\ldots\ldots \text{Eq(5)}$$

Where C_i and Ce (mg/L) are the initial and equilibrium MB concentrations respectively, V (L) is the solution volume and m (g) is the dry adsorbent weight. The effects of contact time, adsorbate and adsorbent concentrations were studied [20].

CHAPTER FOUR

4. RESULTS AND DISCUSSION

4.1 Phytochemicals test

Phytochemical analysis is important to provide information on the classes of compounds present in plant materials that help to determine if there is a secondary metabolite that is used to reduce, cap and stabilize nanoparticles. Based on these results, natural phytochemicals present in leaf extract of the Catha edulis plant was employed as reductants and capping agents in the production of magnetite nanoparticles.

Figure 3 illustrates the result of the phytochemical tests of khat leaf extract. These results indicate the presence of several secondary metabolites, including alkaloids, flavonoids, carbohydrates and tannins. As a result, all tested secondary metabolites (phytochemical compounds) were found in the leaf extract of the Catha edulis plant. T herefore, this metabolite capacity reduces iron oxide through providing electrons, capping and stabilizing the prepared nanoparticles. As example, biomolecules, including proteins, phenolics and flavonoids, are essential for nanoparticle capping and nanoscale ion reduction. Images showing different colour changes during phytochemical screening tests are shown in Fig. 3. This result is consistent with previous literature reports [53].

The colour changes resulting from the study of phytochemicals is a sign that different complexes are formed due to redox reactions. For example, yellow hue of alkaloids suggests that a reaction has occurred between the oxygen or nitrogen atoms of their amide groups. Depending on the nature of the complexes, iron (III) ions generate complexes of different colours in most ferric chloride assays [53].

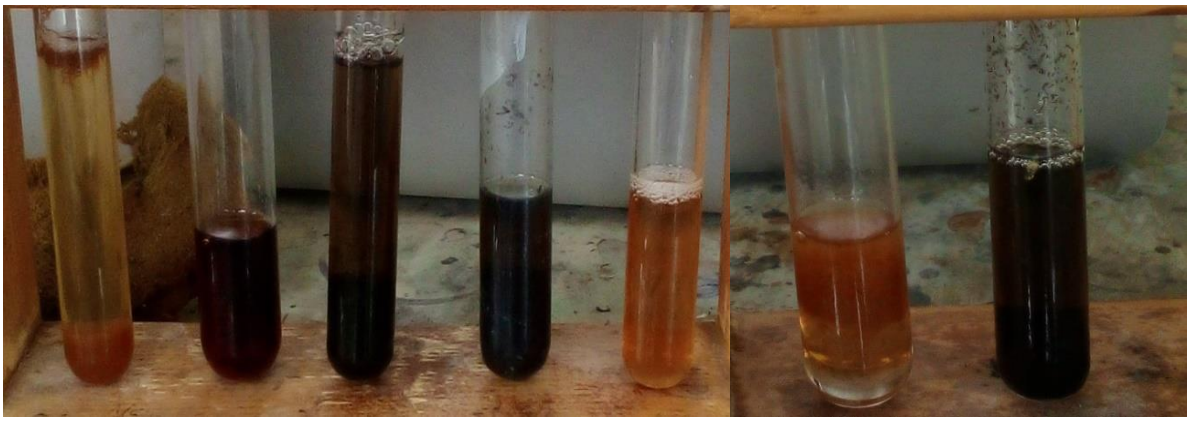

(a) (b) (c) (d) (e) (f) (g)

Figure 3: Colour changes during phytochemical test of Khat leaf extract (a) Alkaloids, (b) Glycosides, (c) flavonoids, (d) Polyphenols, (e) saponins, (f) steroids, and (g). Tannins

4.2 Characterization of (magnetite) Fe_3O_4 NPs

4.2.1 UV-Vis DRS analysis of Fe_3O_4 NPs

Diffuse reflectance measurements were needed to examine optical characteristics and band gap energy of green synthesized magnetite nanoparticle utilizing leaf extract from the Catha edulis plant, as shown in figure 4. The UV-Vis spectrum of green synthesized magnetite nanoparticles revealed the process of reduction and formation of nanoparticles. Magnetite nanoparticle was confirmed by the immediate colour change in the reaction mixture from light yellow to dark brown after addition of Catha edulis plant leaf extract, this was confirmed by the appearance of a strong peak at 364 nm of the magnetite (Fe_3O_4) NPs.

Kubelka–Munk model is used to determine the band gap energy (E_g) of synthesized magnetite nanoparticles using the following equation:

$$F(R) = \frac{(1-R)^2}{2R} \quad \text{..... Eq(6)}$$

Where F(R) is the Kubelka-Munk function, and R is the reflectance. The lowest energy necessary to excite an electron to a state in the conduction band to take part in conduction denotes the band gap [50].These band gap results indicates that the band gap energy of the Fe_3O_4 (1:2 ratio) nanoparticles is 2.54 eV. Magnetite (Fe_3O_4) NPs in 1:2 volume ratios have larger band gap energy, and these results indicate that the band gap energy of magnetite NPs may be particle

size-dependent. This can be described as size of particle reaches the nanoscale, the number of overlapping orbitals or energy levels reduces, and band thickness becomes thinner due to the increasing of the band gap energy between the conduction band and the valence band [54].

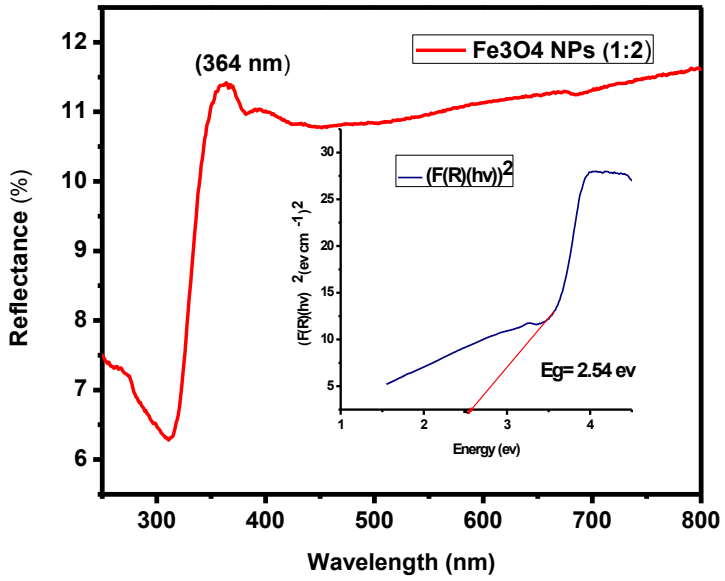

Figure 4: Uv-DRS spectra of Fe_3O_4 NPs (1:2 ratios) and its corresponding band gap energy

4.2.2 **X-ray Diffraction (XRD) analysis**

XRD investigation can be utilized to examine the phase purity and crystallinity of the produced magnetite nanoparticles. The XRD pattern of the synthesized magnetite sample shows six main peak positions and intensity distributions, as shown in the figure. For the produced magnetite nanoparticles (Fe_3O_4 NPs), the diffraction peak was detected at 2θ = 30.33°, 35.35°, 43.27°, 53.72°, 57.14° and 62.10°. These values of (220), (311), (400), (422), (511) and (440) are corresponding to the crystal plane. The diffraction peak of the synthesized Fe_3O_4 NPs was found to be in good agreement with JCPDS paper number 00-019-0629, indicating that no secondary phase was formed during the synthesis of pure Fe_3O_4 Nps. The Fe_3O_4 nanoparticle produced in green appears to have a higher degree of crystallinity, and the absence of detectable impurities by XRD in this sample further confirms the purity of the magnetite (Fe_3O_4) nanoparticles.

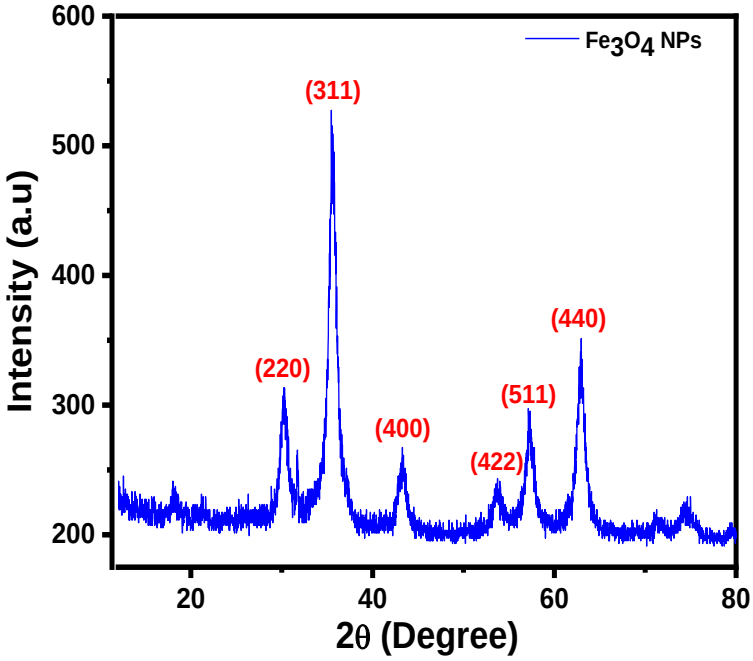

Figure 5: XRD Spectrum of green synthesized Fe_3O_4 NPs

The crystal size of the green-produced magnetite (Fe_3O_4) nanoparticle was determined using Debye-Scherrer equation. The green synthesized magnetite (Fe_3O_4) nanoparticles with the greatest intensity peak had a crystal size of 9 nm, which is represented in the table below.

Table 1: crystallite sizes of synthesized magnetite (Fe_3O_4) NPs.

Sample name	Peak position (2 theta)	FWHM (deg)	Crystal size D(nm)	Average D (nm)
Magnetite NPs (Fe_3O_4)	30.337	0.8817	8.39332306	9.0547516
	35.35	1.022	8.240562342	
	43.27	0.93	9.191871253	
	53.72	0.891	10.01476042	
	57.142	0.97	9.423742576	
	62.10	1.035	9.064250358	

4.2.3 **Fourier transform infrared analysis**

FTIR spectra of a leaf extract from the Catha edulis plant and green-produced magnetite nanoparticles are shown below in Figure 6. The FTIR spectra of Green synthesized magnetite

nanoparticles (Fig. 6) revealed peaks at 3225 cm^{-1}, 1569 cm^{-1}, 1343 cm^{-1}, 1071 cm^{-1}, 551 cm^{-1}, and 430 cm^{-1}. The existence of alcohol and phenol with an O-H stretch is suggested through a significant absorption peak at 3225 cm^{-1}, as demonstrated by specified peaks. The carbonyl group C=C (1550-1650) is seen as a band at 1569 cm^{-1}[50]. The vibrational stretching of carboxylate group (C=O) is shown in a peak at 1343 cm^{-1}. The peak that forms at around 1070 cm^{-1} is due to the vibrational stretching of COO in flavonoids and carboxylic compounds. The two-absorption band at 551 $cm^{-1}$and 430 cm^{-1} corresponds to the bonds of Fe-O in tetrahedral and octahedral sites to approve the spinel-type structure of pure magnetite nanoparticles.

The FTIR spectrum of Catha edulis plant leaf extract is shown in Figure 6. The vibrational range of phenolic molecules and alcohol -OH is showed by the high absorption peak at 3267 cm-1. The vibration stretching of alkene or aromatic C=O bending is responsible for the peak at 1636 cm-1. The C=C bending of alkene and the weak C≡C stretching vibration of alkyne were represented by the peaks at 2100 and 580 cm-1, respectively (Figure 6). Magnetite (Fe_3O_4) NPs can be reduced and capped by the presence of these biologically active plant chemicals. These functional groups showed that the Catha edulis plant extract was reduced and well covered on the surface of the nanomaterial. These outcomes were comparable to the former study on the fabrication of magnetite (Fe_3O_4) nanoparticles via diverse plant extracts [55].

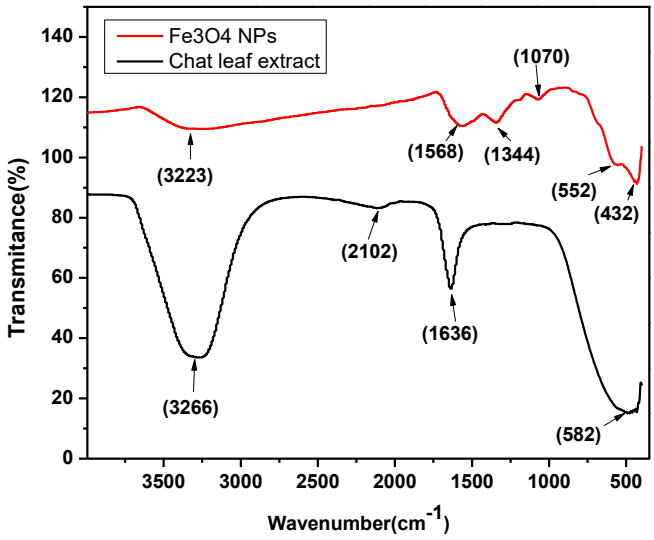

Figure 6: FTIR spectra of green synthesized Fe_3O_4 NPs and Khat leaf extract

4.2.4 SEM analysis of Fe_3O_4 NPs

The surface morphology of the green synthesized Fe_3O_4 NPs adsorbent was examined using a scanning electron microscope (SEM) at different magnifications. The SEM image structure and morphology of the Fe_3O_4 NPs adsorbent before adsorption, as shown in Figure 7, revealed deep empty pores of various sizes and shapes on the surface. The generated Fe_3O_4 NPs exhibited a variety of morphologies and microstructural features for the Fe_3O_4 nanopowder. Furthermore, the SEM images of the Fe_3O_4 NPs showed that the morphology of the nanoparticles was uniform in structure. The observation from some larger nanoparticles can be attributed to the fact that magnetite nanoparticles tend to aggregate because of their high surface energy and high surface tension of ultrafine nanoparticles [55]. Small particle size creates a large superficial area which improves the catalytic activity of the nanoparticles.

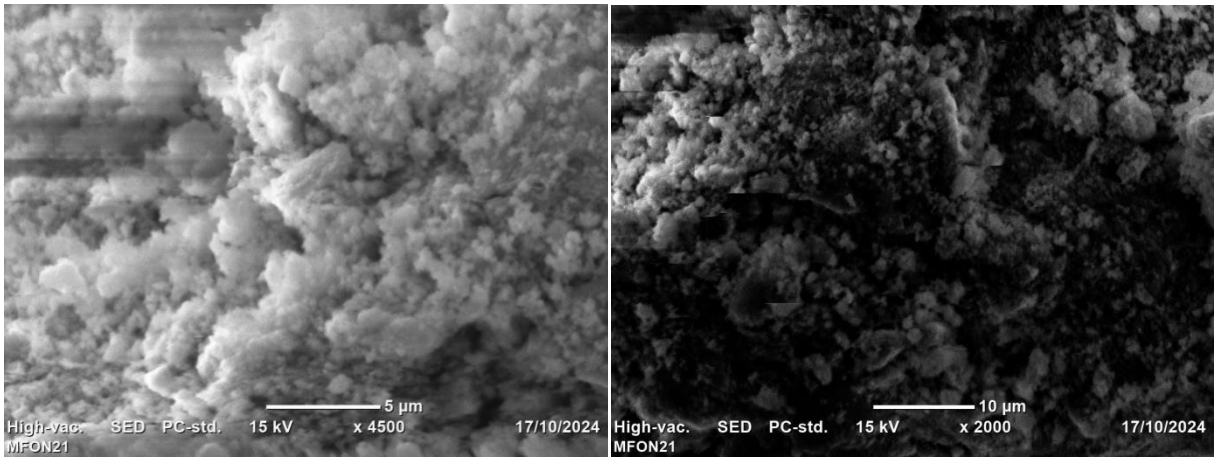

Figure 7: SEM images of green synthesized magnetite (Fe_3O_4) nanoparticles

4.3 Optimization of adsorbent for removal efficiency of methylene blue from aqueous solution

4.3.1 Calibration plot of working methylene blue standard solution

The standardization plot for MB dye at 664 nm is used to determine the residual concentration in the filtrate after the adsorption of MB dye using the synthesized magnetite adsorbent from an aqueous solution. The obtained data from the calibration plot is given in Table 3 and figure 8.

Table 3: Methylene blue dye working standard solution calibration data

Initial concentration of MB(mg/L)	Absorbance
5	0.013
10	0.027
15	0.039
20	0.052

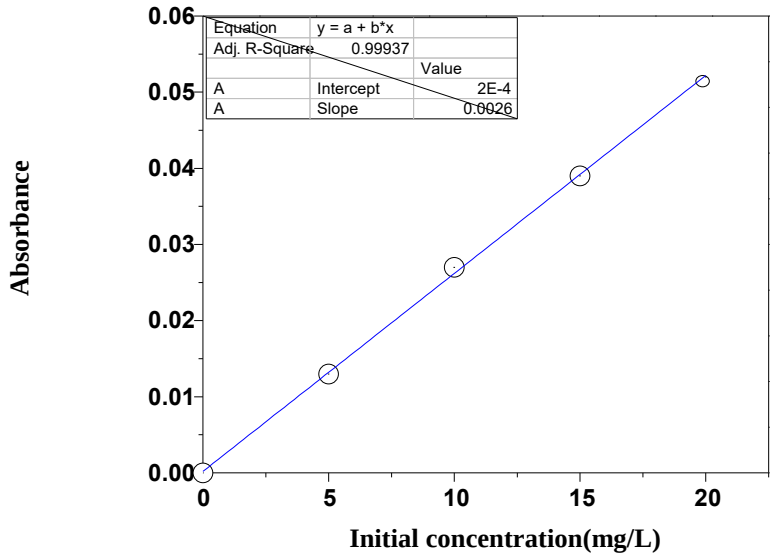

Figure 8: Calibration plot of working methylene blue standards solution.

4.4 MB dye adsorption by using magnetite (Fe_3O_4) NPs

4.4.1 Effect of pH

Due to the surface charge of the adsorbent, the degree of dissociation of the materials in the solution and separation of functional groups at the activated sites of the adsorbent, the pH of the dye solutions is decisive for the adsorption process and, in particular, for the adsorption ability. By introducing 40 mg of magnetite NPs into 10 mg/L of methylene blue solution with pH values from 3 to 9 for a contact time of 50 min, a synthetic adsorbent was used to study the effect of pH on dye adsorption. The pH of the solution was adjusted with 0.1 M HCl or 0.1 M NaOH solutions and the removal of methylene blue dye was examined. As shown in Figure 9, the dye adsorption by magnetite nanoparticles increases with increasing solution pH, because for cationic dyes such as MB, adsorption decreases at pH below pHpzc due to the cationic nature of the adsorbent surface and increases at pH values above pHpzc due to the anionic nature of the

adsorbent surface [56]. In this study, MB adsorption increased by increasing the pH, and its removal capacity increased from pH 3 = (18.50 %) to pH 9 = (85.18%).

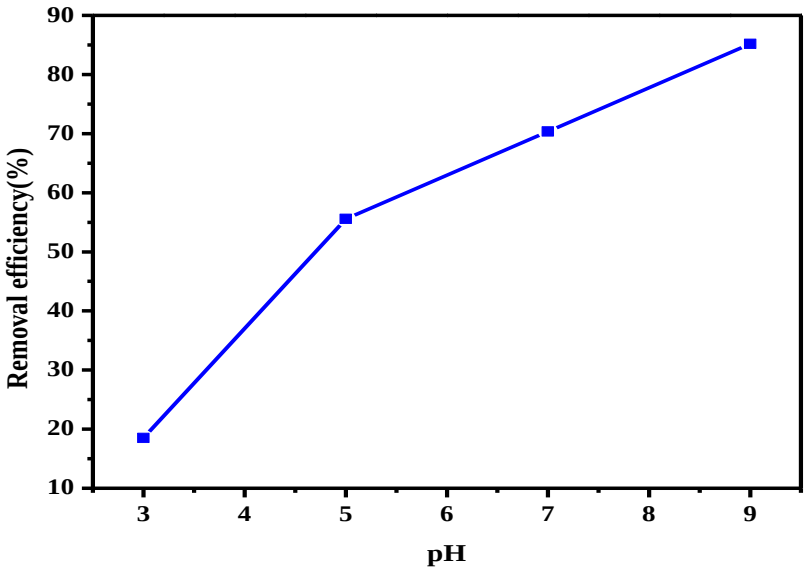

Figure 9: Effect of pH on MB dye removal by magnetite NPs

4.4.2 **Effect of adsorbent dosage**

To study the influence of the dosage of magnetite NP adsorbent at pH 9, MB dye was used at a fixed concentration of 10 mg/L for 50 min. For this experiment, an adsorbent with different dosages (20-80 mg) was used for the generated samples. Figure 10 illustrates how different adsorbent dosages influence the removal of MB by the selected magnetite NPs. The results show that when the amount of adsorbent was increased to 80 mg, the percentage of MB dye removal decreased from 96.30% to 37.05% on this magnetite adsorbent. This is due to a decrease in the adsorption sites. Further increases in adsorbent dosage did not improve dye removal; this is because all available adsorption sites had reached saturation and were no longer available to the dye molecules for adsorption [57]. Thus, the optimal concentration of nanoparticles was found to be 20 mg, and this amount was used for subsequent experimental analysis.

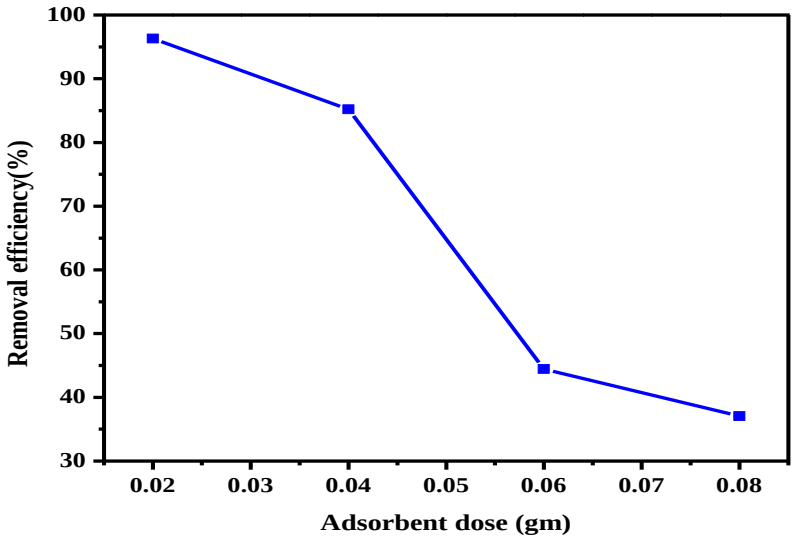

Figure 10: Effect of adsorbent dose on the removal of MB dye by magnetite NPs

4.4.3 **Effect of contact time**

One of the most important factors in the development of economical wastewater treatment systems is the equilibrium time. Figure 11 illustrates how methylene blue dye was adsorbed at an initial concentration of 10 mg/L over a range of contact times (30 to 90 min) with a 20 mg dose of a magnetic adsorbent produced at pH 9. According to the data, it takes only 50 min to reach equilibrium conditions. Many activated adsorption sites that are open to dye molecules and increase dye penetration on the adsorption surface are the reason for the high adsorption rate at the initial contact times. Saturation of the adsorbent surface causes the concentration gradient to decrease with time, but the percent removal remains essentially constant. During the first 30 min adsorption period to the 50 min equilibrium period, the percentage of dye removal was increased from 33.35% to 96.60% for magnetite nanoparticles. This is due to the availability of a large number of free adsorption sites during the initial phase of the reaction. As these sites become occupied the rate of adsorption decreases over time and the system reaches equilibrium at 50 minutes [58].

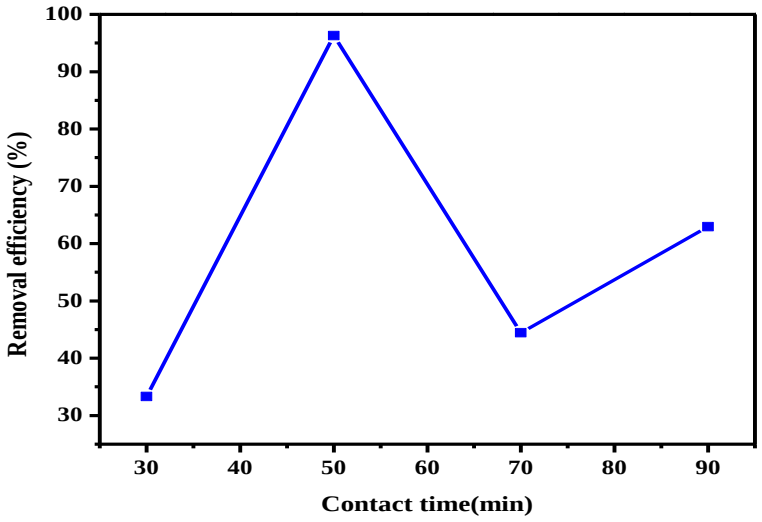

Figure 11: Effect of contact time on the removal of MB dye by magnetite NPs

4.4.4 **Effect of initial concentration**

To study the effect of the initial dye concentration on the adsorption properties, a series of experiments were conducted using different concentrations of MB solution (5, 10, 15 and 20 mg/L) with an adsorbent dose of 20 mg of magnetite nanoparticles at pH 9 within 50 minutes of contact time. As shown in Figure 12, the adsorption is very fast at a lower initial concentration of MB solution. The result shows that the removal efficiency decreases with an increase in initial concentrations, although the total amount of MB accumulation increases. From this experiment, it was observed that about 99.25% of MB was removed at an initial concentration of 5 mg/L with the adsorbent magnetite nanoparticles shown in Figure 12. The MB removal percentage decreased with the increase of initial dye concentration, which may be due to the saturation of adsorption sites on the adsorbent surface. At a low initial concentration, there will be unoccupied active sites on the adsorbent surface, because most of the MB solution can contact the active sites of the adsorbent [58].

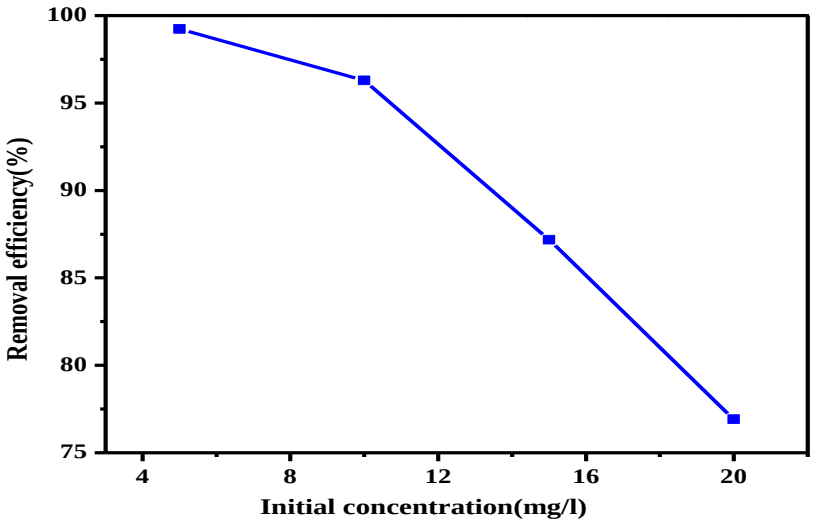

Figure 12: Effect of initial concentration on MB dye removal by magnetite NPs

4.5 Adsorption isotherm

When equilibrium is reached during adsorption, the retained particles spread between the liquid phase and the solid surface, as shown by the adsorption isotherm. A crucial step in selecting the right model is to examine the isotherm data by fitting it to different isotherm models. Freundlich and Langmuir adsorption isotherms were used to investigate the synthesized magnetite (Fe_3O_4) nanoparticle adsorbent in the context of the adsorption isotherm model [59].

4.5.1 Langmuir adsorption isotherm model

The development of uniform monolayer coverage on the adsorbent surface, uniform adsorption energy, and the absence of molecular interactions between adsorbed molecules at adjacent sites are the foundations of the Langmuir adsorption isotherm. The amount of dye adsorbed per unit mass of adsorbent (q_e) and the dye concentration in equilibrium solution (C_e) can be used to study adsorption isotherms. In this study, the slope and intercept of a linear form of the Langmuir equation was used to determine the Langmuir constant (KL) and the maximum adsorption capacity (qmax), respectively [59].

$$\frac{Ce}{qe} = \frac{Ce}{q_{max}} + \frac{1}{q_{max}K_L} \quad \text{Eq(7)}$$

The plot of C_e versus C_e/q_e allowed for the determination of the values of q_{max} (mg/g) and KL (L/mg). Changes in the surface area and porosity of the adsorbent are often associated with

adsorption capacity. Adsorption capacity increases with increasing surface area and pore volume [60]. The equilibrium parameter, or RL, is a dimensionless constant commonly used to explain the fundamental properties of the Langmuir isotherm model.

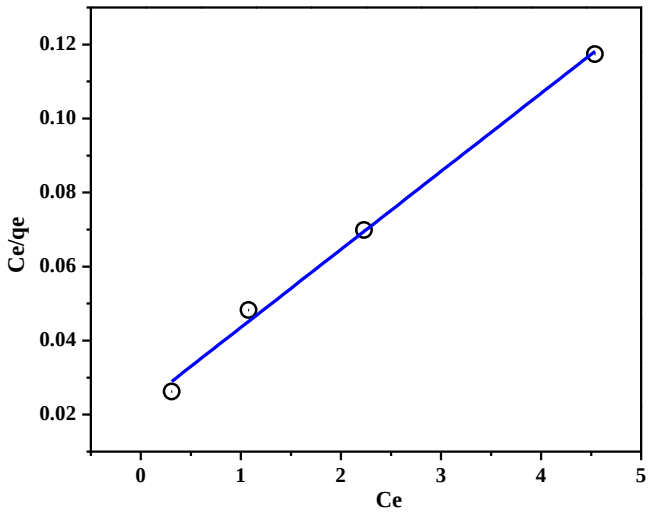

Figure 13: Langmuir adsorption isotherm model for magnetite NPs adsorbent

Langmuir isotherm model	synthesized samples
	Fe_3O_4
q_{max}(mg/g)	44.65
R_L	0.15
K_L (L/mg)	1.06
R^2	0.995

Table 4: Parameters of Langmuir isotherm models for synthesized sample

Langmuir adsorption was indicated by the maximum adsorption capacity (q_{max}), which represents the adsorption of the saturated monolayer at equilibrium. The result presented in Table 4 shows that the Langmuir adsorption isotherm parameters q_{max} (44.65 mg/g) and R^2 were 0.995 for magnetite nanoparticles. According to the Langmuir correlation coefficient R^2, the adsorption isotherm shows that the adsorption study of MB dye on magnetite nanoparticles was better fitted

linearly by the Langmuir isotherm model than by Freundlich. The calculated values of the absorption energy constant a (KL) is 1.06 L/mg. This shows that the adsorption efficiency of the adsorbent was good, because its KL value was smaller. According to the Langmuir model, RL values calculated as 0.15 were obtained between 0 and 1 for the magnetite adsorbent, which confirmed that adsorbents that adsorb MB from aqueous solution are favorable under the conditions applied in this study.

4.5.2 **Freundlich adsorption isotherm model**

The Freundlich isotherm model is the first known relationship that describes non-ideal and reversible adsorption without being limited to the formation of a single layer. This empirical model can be applied to multilayer adsorption with a non-uniform distribution of the heat of adsorption and affinity on the heterogeneous surface [61]. The linear form of the Freundlich isotherm equation is as follows:

$$\ln \mathrm{qe} = \ln Kf + \frac{1}{n} \ln Ce \ldots\ldots\ldots\ldots\ldots\ldots\ldots\ldots\ldots \text{Eq(8)}$$

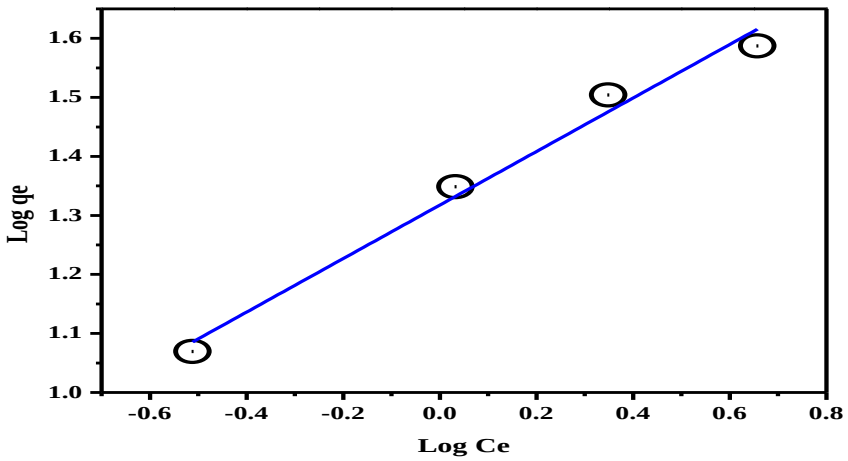

Figure 14: Freundlich adsorption isotherm models for magnetite (Fe_3O_4) NPs.

A higher adsorption mechanism and the development of a significantly stronger bond between the adsorbate and the adsorbent are indicated by a lower value of Freundlich equation coefficient, 1/n. The Value of 1/n less than 1 suggest that bond energies increase with surface density. Conversely, value greater than 1 indicates a decrease in bond energies with increasing

surface density. A 1/n value of 1 implies uniform adsorption across all surface sites. For this study, the 1/n value for MB dye adsorption fell within the typical range of 1–10, showing favorable adsorption [62].

The results of the isotherm parameters are shown in Table 5. The 1/n value of the Freundlich parameter, which shows how favorably MB dye adsorption occurs on magnetite (Fe_3O_4) NPs adsorbent, was between 0 and 1. This implies that the binding between the MB dye and the produced adsorbents was strong because the value of (n) is greater than 1. The favorable adsorption process is indicated by the computed values of the Freundlich equation coefficient n (n = 2.22) in this investigation, which are greater than 1. Furthermore, for the synthesized NPs adsorbent, the Freundlich correlation coefficient (R^2) was 0.979. This suggests that the Langmuir isotherm correlation coefficient of the biosynthesized adsorbent was higher than the Freundlich isotherm correlation coefficient R^2. This suggests that the experimental data of the magnetite adsorbent are not fit to the Freundlich isotherm model. Table 5 below presents the values of the Freundlich isotherm parameters and constants.

Table 5: Freundlich isotherm model parameters for synthesized samples

Freundlich isotherm model	synthesized samples
	Fe_3O_4
K_F(mg/g)	20.77
(n)	2.22
1/n	0.45
R^2	0.979

4.6 Adsorption kinetics study

4.6.1 Pseudo-first order kinetics model

Pseudo-first order kinetics is determined using the following equation.

$$\ln (q_e - q_t) = lnq_e - K_1 \text{ x } t \quad \text{..... Eq(9)}$$

Where q_e (mg/g) and q_t (mg/g) are the mass of MB adsorbed at equilibrium and at time t, respectively. K_1 is the first-order rate constant of adsorption. A straight line of log (q_e-q_t) versus t tells the applicability of this kinetics model (Figures 15); q_e and K_1 were determined from the intercept and slope of the plot, respectively (Table 8). For MB dye, it was discovered that the values of q_e and K_1 were 1.2044 and 0.022, respectively. Table 8 shows that the value of R^2 for this model under study was 0.67866 for MB dye. The pseudo-first-order kinetics model is poor correlation coefficient values show that adsorption takes place at more than one location per ion.

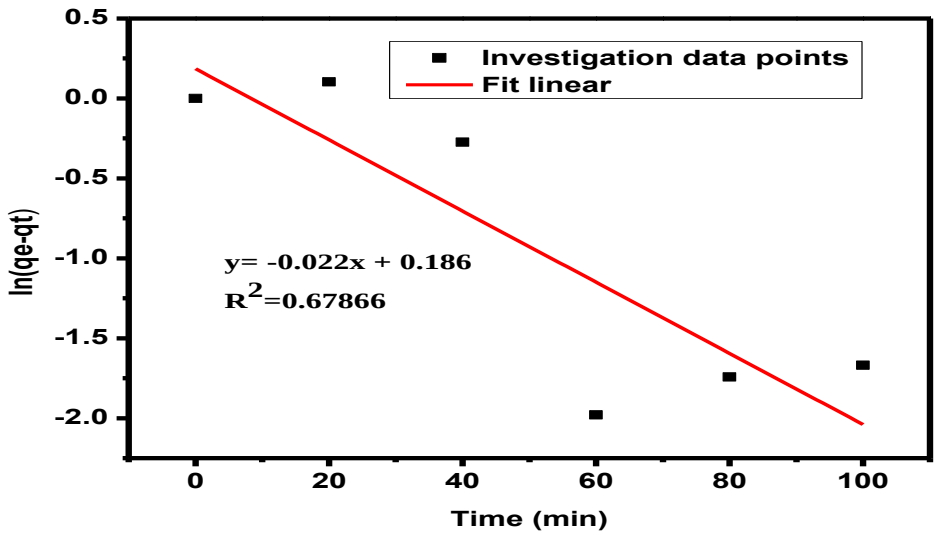

Figure 15: Pseudo first-order adsorption kinetics of MB dye on magnetite nanoparticle

4.6.2 **Pseudo-second order kinetics model**

Pseudo second order kinetics model describes the adsorption process over the entire contact time range. The pseudo-second order kinetics is determined using the following equation.

$$\frac{t}{qt} = \frac{1}{k2\, qe^2} + \frac{t}{qe} \quad \text{..... Eq(10)}$$

Where, q_t is MB adsorbed per unit mass of adsorbent (mg/g) at time t, q_e is the MB adsorbed per unit mass of adsorbent (mg/g) at equilibrium, and k_2 (g/mg.min) is the rate constants of pseudo second order kinetics equations.

Slope and intercept of the plot of t/q_t vs t as shown in Figure 15 were used to calculate qe (mg/g) and K_2 (g/mg min), which were determined to be 3.268 and 0.0544, respectively. The equilibrium adsorption capacity values of pseudo-second-order kinetics, q_e (calc), were determined to be 3.268. It was discovered that the pseudo-second-order kinetics model had higher regression coefficient value (R^2=1) than the pseudo-first-order kinetics model (R^2=0.67866). The regression coefficient value (R^2 = 1) of pseudo-second-order kinetics, is higher than pseudo-first-order kinetics, as shown in Figure 16 and Table 8, which indicates that the adsorption follows pseudo-2nd order adsorption process. The obtained result demonstrated that the sorption capacity is directly proportional to the number of active sites on the sorbent and that the rate-controlling step of MB dye adsorption on Fe_3O_4 NPs involves chemisorption [63].

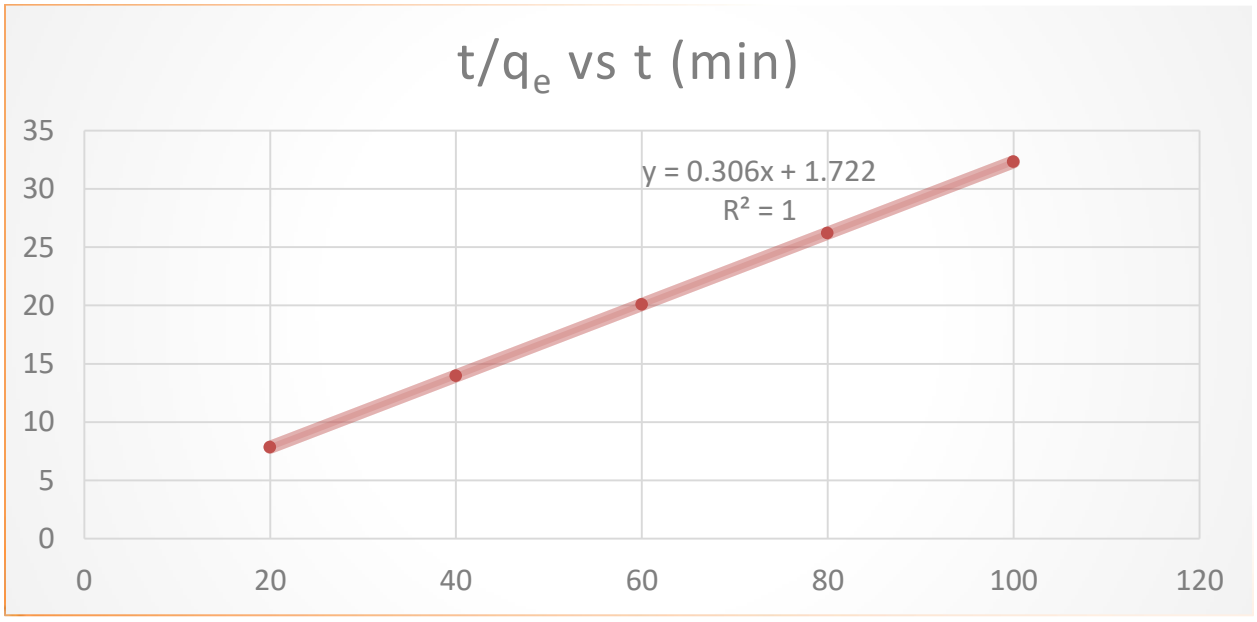

Figure 16: Pseudo-second order adsorption kinetics of MB dye on magnetite nanoparticle

Table 6: Adsorption kinetics constants at the same concentrations

Dye	Pseudo first order kinetics model				Pseudo second order kinetics model			
MB	q_e (mg/g)	q_{e1}	k_1	R^2	q_e (mg/g)	q_{e2}	K_2	R^2
	3.25932	1.2044	0.022	0.67866	3.25932	3.268	0.0544	1

CHAPTER FIVE

5. CONCLUSION AND RECOMMENDATIONS

5.1 Conclusion

A study was investigated to assess the effectiveness of green synthesized magnetite nanoparticles in removing methylene blue (MB) dye from aqueous solution. Magnetite nanoparticles were produced using a plant leaf extract of Catha edulis species as a reducing and stabilizing agent. Magnetite (Fe_3O_4) nanoparticles had an average crystallite size of 9.05 nm and a face-centered cubic structure, as determined by XRD analysis. FTIR analysis confirmed that the green manufacturing process produced the nanoparticles and that the active metabolites contained in the khat leaf extract were facilitated the reduction of Fe_3O_4 nanoparticles. The synthesized Fe_3O_4 nanoparticles exhibited a variety of morphologies and microstructural features for nanoscale Fe_3O_4 powder. Furthermore, SEM images of Fe_3O_4 nanoparticles showed that the morphology of the nanoparticles was uniform in structure. The development of magnetite nanoparticles facilitated adsorption in the visible region, as shown by UV-Vis fluorescence spectroscopy. The efficiency of the adsorbent was examined using a batch adsorption experiment for different factors such as initial concentration, adsorbent dosage, contact time, and pH. Room temperature studies were performed for all optimization parameters of the magnetite adsorbent. MB dye adsorption of Fe_3O_4 nanoparticles was extremely sensitive to PH. The optimized conditions for methylene blue dye removal using synthesized magnetite nanoparticles were determined to be pH 9, an adsorbent dose of 20 mg, a contact time of 50 minutes and initial dye concentration of 5 mg/L. Under these optimized conditions, the magnetite nanoparticles achieved MB removal efficiency of 99.25%. In the adsorption process of Fe_3O_4 nanoparticles, the Langmuir isotherm model provided a superior fit to the Freundlich isotherm model ($R^2 = 0.995$ vs. $R^2 = 0.979$). Furthermore, the pseudo-second-order kinetic model better represented the adsorption kinetics than the pseudo first order kinetics ($R^2 = 1$ vs. $R^2 = 0.67866$). These findings indicate that the green-synthesized magnetite nanoparticles are a highly effective and environmentally friendly adsorbent for treating dye-contaminated water.

5.2 Recommendation

The following recommendations are offered to assist individuals who wish to focus on this area of study in light of the recent discovery of Fe_3O_4 nanoparticles created utilizing leaf extract of khat intended for methylene blue adsorption. The synthesized samples should be characterized by energy dispersive x-ray (EDX) to determine the elemental composition of the nanoparticle. To study the particle size, more detailed morphology, and surface area of the nanoparticles, the samples should be characterized by Transmission electron microscopy and Brunauer-Emmett-Teller instruments, respectively. Further studies in this area are needed to utilize magnetite nanoparticles on an industrial and commercial scale.

REFERANCE

1. Saravanan, A., Kumar, P. S., Karishma, S., VO, D. V. N., Jeevanantham, S., Yaashikaa, P., & George, C. S. (2021), 'A review on biosynthesis of metal nanoparticles and its environmental applications,' *Chemosphere, 264*:p.128580.
2. Zafar, R., Bashir, S., Nabi, D., &Arshad, M. (2021), 'Occurrence and quantification of prevalent antibiotics in wastewater samples from Rawalpindi and Islamabad, Pakistan,'*Science of The Total Environment, 764*:p.142596.
3. Konicki, W., Aleksandrzak, M., & Mijowska, E. (2017). Equilibrium, kinetic and thermo dynamic studies on adsorption of cationic dyes from aqueous solutions using graphene oxide. *Chemical Engineering Research and Design, 123*, 35 to 49.
4. Aboelfetoh, E. F., Gemeay, A. H., & El-Sharkawy, R. G. (2020). Effective disposal of methylene blue using green immobilized silver nanoparticles on graphene oxide and reduced graphene oxide sheets through one-pot synthesis. *Environmental Monitoring and Assessment, 192*(6).
5. Mohan, D., & Pittman Jr., C. U. (2006), 'Activated carbons and low cost adsorbents for remediation of tri- and hexavalent chromium from water,' *Journal of Hazardous Materials, 137*(2):p.762–811.
6. Aksu, Z., &Kutsal, T. (2007),'A bioseparation process for removing lead (II) ions from waste water by using C. vulgaris,'*Journal of Chemical Technology & Biotechnology*, *52*(1):p. 109–118
7. Das, C., Sen, S., Singh, T., Ghosh, T., Paul, S. S., Kim, T. W., Jeon, S., Maiti, D. K., Im, J., &Biswas, G. (2020),' Green Synthesis, Characterization and Application of Natural Product Coated Magnetite Nanoparticles for Wastewater Treatment,' *Nanomaterials, 10*(8):p.1615.
8. Soares, P. I., Laia, C. A., Carvalho, A., Pereira, L. C, Coutinho, J. T., Ferreira, I. M., Novo, C. M., & Borges, J. P. (2016), 'Iron oxide nanoparticles stabilized with a bilayer of oleic acid for magnetic hyperthermia and MRI applications,' *Applied Surface Science, 383*:p.240–247.

9. Zhang, S., Zhang, Y., Bi, G., Liu, J., Wang, Z., Xu, Q., Xu, H., & Li, X. (2014), 'Musselinspired polydopamine biopolymer decorated with magnetic nanoparticles for multiple pollutants removal,' *Journal of Hazardous Materials, 270*:p.27–34.
10. Kolhatkar, A., Jamison, A., Litvinov, D., Willson, R., & Lee, T. (2013), 'Tuning the Magnetic Properties of Nanoparticles,' *International Journal of Molecular Sciences, 14*(8):p.15977.
11. Welderfael, T., Yadav, O., Taddesse, A., &Kaushal, J. (2013), 'Synthesis, characterization and photo catalytic activities of Ag-N-codopedZnO nanoparticles for degradation of methyl red,' *Bulletin of the Chemical Society of Ethiopia, 27*(2).
12. Nimkar, U. (2018). Sustainable chemistry: A solution to the textile industry in a developi ng world. *Current Opinion in Green and Sustainable Chemistry, 9,* 13 to 17.
13. Jain, K., Patel, A. S., Pardhi, V. P., & Flora, S. J. S. (2021),' Nanotechnology in Wastewater Management: A New Paradigm towards Wastewater Treatment,'*Molecules, 26*(6):p.1797
14. Bouafia, A., &Laouini, S. E. (2021), 'Plant-Mediated Synthesis of Iron Oxide Nanoparticles and Evaluation of the Antimicrobial Activity: A Review,' *Mini-Reviews in Organic Chemistry, 18*(6):p. 725–734.
15. Kumavat, S. R., & Mishra, S. (2021),' Green synthesis of silver nanoparticles using Borago officinal is leaves extract and screening its antimicrobial and antifungal activity. *International Nano Letters*,'*11*(4):p.355–370.
16. Sallak, N., MotallebiMoghanjoughi, A., Ataee, M., Anvar, A., &Golestan, L. (2021), 'Antimicrobial biodegradable film based on corn starch/Saturejakhuzestanica essential oil/Ag–TiO2 nanocomposites,' *Nanotechnology, 32*(40):p.405-703.
17. Cheriyamundath, S., &Vavilala, S. L. (2020),' Nanotechnology-based wastewater treatment Water *and Environment Journal, 35*(1):p. 123–132
18. Mohammadi, H., Nekobahr, E., Akhtari, J., Saeedi, M., Akbari, J., &Fathi, F. (2021), 'Synthesis and characterization of magnetite nanoparticles by co-precipitation method coated with biocompatible compounds and evaluation of in-vitro cytotoxicity,' *Toxicology Reports, 8*:p.331–336.
19. Gupta, A. K., & Gupta, M. (2005),' Synthesis and surface engineering of iron oxide nanoparticles for biomedical applications,' *Biomaterials, 26*(18):p.3995–4021.

20. Namdeo, M. (2018), ’Magnetite Nanoparticles as Effective Adsorbent for Water Purification-A Review,’ *Advances in Recycling & Waste Management*, *02*(03).
21. Beiki, S, Moniri, E., Hassani, A. H., & Ahmad Panahi, H. (2020), ‘Preparation and Characterization of Dendrimer-Modified Magnetite Nanoparticles for Adsorption of Humic Acid from Aqueous Solution,’*ChemistrySelect*, *5*(24):p. 7197–7204.
22. Bogunia-Kubik, K., &Sugisaka, M. (2002), ‘From molecular biology to nanotechnology and nanomedicine,’ *Biosystems*, *65*(2–3):p.123–138
23. Chin, A. B., &Yaacob, I. I. (2007),’Synthesis and characterization of magnetic iron oxide nanoparticles via w/o micro emulsion and Massart’s procedure,’ *Journal of Materials Processing Technology*, *191*(1–3):p.235–237.
24. Han, L. H., Liu, H., & Wei, Y. (2011),’ In situ synthesis of hematite nanoparticles using a low temperature micro emulsion method,’ *Powder Technology*, *207*(1–3):p.42–46.
25. Joseyphus, R. J., Kodama, D., Matsumoto, T., Sato, Y., Jeyadevan, B., &Tohji, K. (2007), ’Role of polyols in the synthesis of Fe particles,’ *Journal of Magnetism and Magnetic Materials*, *310*(2):p.2393–2395.
26. Cai, W., & Wan, J. (2007), ‘Facile synthesis of super paramagnetic magnetite nanoparticles in liquid polyols,’ *Journal of Colloid and Interface Science*, *305*(2):p.366–370.
27. Abbas, M., Parvatheeswara Rao, B., Naga, S., Takahashi, M., & Kim, C. (2013), ‘Synthesis of high magnetization hydrophilic magnetite (Fe3O4) nanoparticles in single reaction Surfactant less polyols process, ’*Ceramics International*, *39*(7):p. 7605–7611.
28. Abu Mukh-Qasem, R., &Gedanken, A. (2005),‘Sonochemical synthesis of stable hydrosol of Fe_3O_4 nanoparticles,’ Journal *of Colloid and Interface Science*, *284*(2):p.489–494.
29. Park, S. J., Kim, S., Lee, S., Khim, Z. G., Char, K., &Hyeon, T. (2000), ’Synthesis and Magnetic Studies of Uniform Iron Nanorods and Nanospheres,’ *Journal of the American Chemical Society*, *122*(35), 8581–8582.
30. Hee Kim, E., Sook Lee, H., Kook Kwak, B., & Kim, B. K. (2005),’ Synthesis of ferrofluid with magnetic nanoparticles by sonochemical method for MRI contrast agent,’*Journal of Magnetism and Magnetic Materials*, *289*:p.328–330.

31. Kumfer, B. M., Shinoda, K., Jeyadevan, B., & Kennedy, I. M. (2010),' Gas-phase flame synthesis and properties of magnetic iron oxide nanoparticles with reduced oxidation state,' *Journal of Aerosol Science, 41*(3):p.257–265.
32. Martínez-Mera, I., Espinosa-Pesqueira, M., Pérez-Hernández, R., & Arenas-Alatorre, J. (2007), 'Synthesis of magnetite (Fe_3O_4) nanoparticles without surfactants at room temperature,' *Materials Letters,61*(23–24):p.4447–4451
33. Li, Y., Hu, Y., Huang, G., & Li, C. (2013), 'Metallic iron nanoparticles: Flame synthesis, characterization and magnetic properties,' *Particuology, 11*(4):p.460–467.
34. Saunders, R. W., & Plane, J. M. (2010), 'The formation and growth of Fe2O3 nanoparticles from the photo-oxidation of iron penta carbonyl. *Journal of Aerosol Science, 41*(5):p.475–489.
35. Cui, H., Liu, Y., &Ren, W. (2013), 'Structure switch between α-Fe_2O_3, γ-Fe_2O_3 and Fe3O4 during the large scale and low temperature sol–gel synthesis of nearly mono dispersed iron oxide nanoparticles,' *Advanced Powder Technology, 24*(1):p.93–97.
36. Marques, R. F., Garcia, C., Lecante, P., Ribeiro, S. J., Noé, L., Silva, N. J., Amaral, V. S., Millán, A., &Verelst, M. (2008),' Electro-precipitation of Fe3O4 nanoparticles in ethanol,'*Journal of Magnetism and Magnetic Materials, 320*(19):p.2311–2315.
37. Cabrera, L., Gutierrez, S., Menendez, N., Morales, M., &Herrasti, P. (2008), 'Magnetite nanoparticles: Electrochemical synthesis and characterization,' *Electrochemical Acta, 53*(8):p. 3436–3441.
38. Fajaroh, F., Setyawan, H., Widiyastuti, W., &Winardi, S. (2012),' Synthesis of magnetite nanoparticles by surfactant-free electrochemical method in an aqueous system,' *Advanced Powder Technology, 23*(3):p.328–333.
39. Laurent, S., Forge, D., Port, M., Roch, A., Robic, C., Vander Elst, L., & Muller, R. N. (2008), 'Magnetic Iron Oxide Nanoparticles: Synthesis, Stabilization, Vectorization, Physicochemical Characterizations, and Biological Applications,' *Chemical Reviews, 108*(6):p. 2064–2110.
40. Yew, Y. P., Shameli, K., Miyake, M., Kuwano, N., Bt Ahmad Khairudin, N. B., BtMohamad, S. E., & Lee, K. X. (2016), 'Green Synthesis of Magnetite (Fe_3O_4) Nanoparticles Using Seaweed (Kappaphycusalvarezii) Extract,' *Nanoscale Research Letters, 11*(1).

41. El-Sheikh, A. H., Fasfous, I. I., Al-Salamin, R. M., & Newman, A. P. (2018),' Immobilization of citric acid and magnetite on sawdust for competitive adsorption and extraction of metal ions from environmental waters,' *Journal of Environmental Chemical Engineering*, *6*(4):p. 5186–5195.
42. Sheshmani, S., &Mashhadi, S. (2017), 'Potential of magnetite reduced graphene oxide/chitosan nanocomposite as biosorbent for the removal of dyes from aqueous solutions,' *Polymer Composites, 39*:p.E457–E462.
43. Thirunavukkarasu, A., Nithya, R., &Sivashankar, R. (2021), 'Continuous fixed-bed biosorption process: A review,' *Chemical Engineering Journal Advances, 8*:p.100188.
44. Tanyildizi MŞ (2011) Modeling of adsorption isotherms and kinetics of reactive dye from aqueous solution by peanut hull. Chem Eng J 168:1234–1240.
45. Tang SCN, Lo IMC (2013) Magnetic nanoparticle: essential factors for sustainable environmental applications. Water Res 47:2613 2632.
46. ŠafaříkováŠafařík MI (1999) Magnetic solid-phase extraction. J Magn Magn Mater 194:108–112.
47. Abate, G. Y., Alene, A. N., Habte, A. T., &Getahun, D. M. (2020a),'Adsorptive removal of malachite green dye from aqueous solution onto activated carbon of Catha edulis stem as a low cost bio-adsorbent, '*Environmental Systems Research*:pp. *9*(1).
48. Chen, Y. G., Ye, W. M., Yang, X. M., Deng, F. Y., & He, Y. (2010),' Effect of contact time, pH, and ionic strength on Cd(II) adsorption from aqueous solution onto bentonite from Gaomiaozi, China,' *Environmental Earth Sciences*, *64*(2):p.329–336.
49. Rajput S., Pittman C. U., Mohan D., (2016), Magnetic magnetite (Fe_3O_4) nanoparticle sy nthesis and applications for lead (Pb2+) and chromium (Cr6+) removal from water. *J. Colloid Interf. Sci*. 468: 334–346
50. Gabal, R. A., Shokeir, D., & Orabi, A. (2022). *Cytotoxicity and Hemostatic One Step Green Synthesis of Iron Nanoparticles Coated with Green Tea for Biomedical Application*. *19*(3).
51. Mahdavi, M., Namvar, F., Ahmad, M. Bin, & Mohamad, R. (2013). *Green Biosynthesis and Characterization of Magnetic Iron Oxide (Fe3O4) Nanoparticles Using Seaweed (Sargassum muticum) Aqueous Extract*. 59545964.

52. Mulushewa, Z., Dinbore, W. T., & Ayele, Y. (2021). Removal of methylene blue from textile waste water using kaolin and zeolite-x synthesized from Ethiopian kaolin. *Environmental Analysis Health and Toxicology*, *36*(1), e2021007.
53. KiflomGebremedhn, Mebrahtu Hagos Kahsay, &Muluken Aklilu. (2019). Green Synthesis of CuO Nanoparticles Using Leaf Extract of *Catha edulis* and Its Antibacterial Activity. *Journal of Pharmacy and Pharmacology*, *7*(6).
54. Singh, M., Goyal, M., & Devlal, K. (2018). Size and shape effects on the band gap of semiconductor compound nanomaterials. *Journal of Taibah University for Science*, *12*(4), 470–475.
55. Kumar, V. (2019). *Green Synthesis and Characterization of Iron Oxide Nanoparticles Using Phyllanthus Niruri Extract*.
56. Das, S. K., Khan, M. M., Parandhaman, T., Laffir, F., Guha, A. K., Sekaran, G., & Mandal, A. B. (2013). Nano-silica fabricated with silver nanoparticles: Antifouling adsorbent for efficient dye removal, effective water disinfection and biofouling control. *Nanoscale*, *5*(12), 5549.
57. Wu, Q., Feng, C., Wang, C., & Wang, Z. (2013). A facile one-pot solvothermal method to produce superparamagnetic graphene–fe3o4 nanocomposite and its application in the removal of dye from aqueous solution. *Colloids and Surfaces B: Biointerfaces*, *101*, 210–214.
58. Elmorsi, T. M. (2011). Equilibrium isotherms and kinetic studies of removal of methylene blue dye by adsorption onto Miswak leaves as a natural adsorbent. *Journal of Environmental Protection*, *02*(06), 817–827.
59. Md Sandollah, N. A., Sheikh Mohd Ghazali, S. A., Wan Ibrahim, W. N., &Rusmin, R. (2020). Adsorption-desorption profile of methylene blue dye on raw and acid activated kaolinite. *Indonesian Journal of Chemistry*, *20*(4), 755.
60. Kavithad, D., &Namasivayam, C. (2007). Experimental and kinetic studies on methylene blue adsorption by Coir Pith Carbon. *Bioresource Technology*, *98*(1), 14–21.
61. Wang, F., Zhang, L., Wang, Y., Liu, X., Rohani, S., & Lu, J. (2017). Fe_3O_4 @SiO_2 @CS-TETA functionalized graphene oxide for the adsorption of methylene blue (MB) and Cu (II). *Applied Surface Science*, *420*, 970981.

62. Salifu, A. (2017). Fluoride removal from drinking water using granular aluminum-coated bauxite as adsorbent: Optimization of synthesis process conditions and equilibrium study. *Fluoride Removal from Groundwater by Adsorption Technology*, 161–202.
63. Pitchay, T., Jawad, A. H., Johari, I. S., & Sabar, S. (2022). Kinetics Studies of Metallic Ions Adsorption by Immobilised Chitosan. *Science Letters*, *16*(1), 137.
64. Chen, W., Li., M., Wang.,L., Zhang,Y.and Wang,J.(2021). Magnetic nanomaterials for waste water treatment: A review. Materials Science and Engineering B, 273,115453.

APPENDIX

Figure 1: catha edulis plant leaf drying

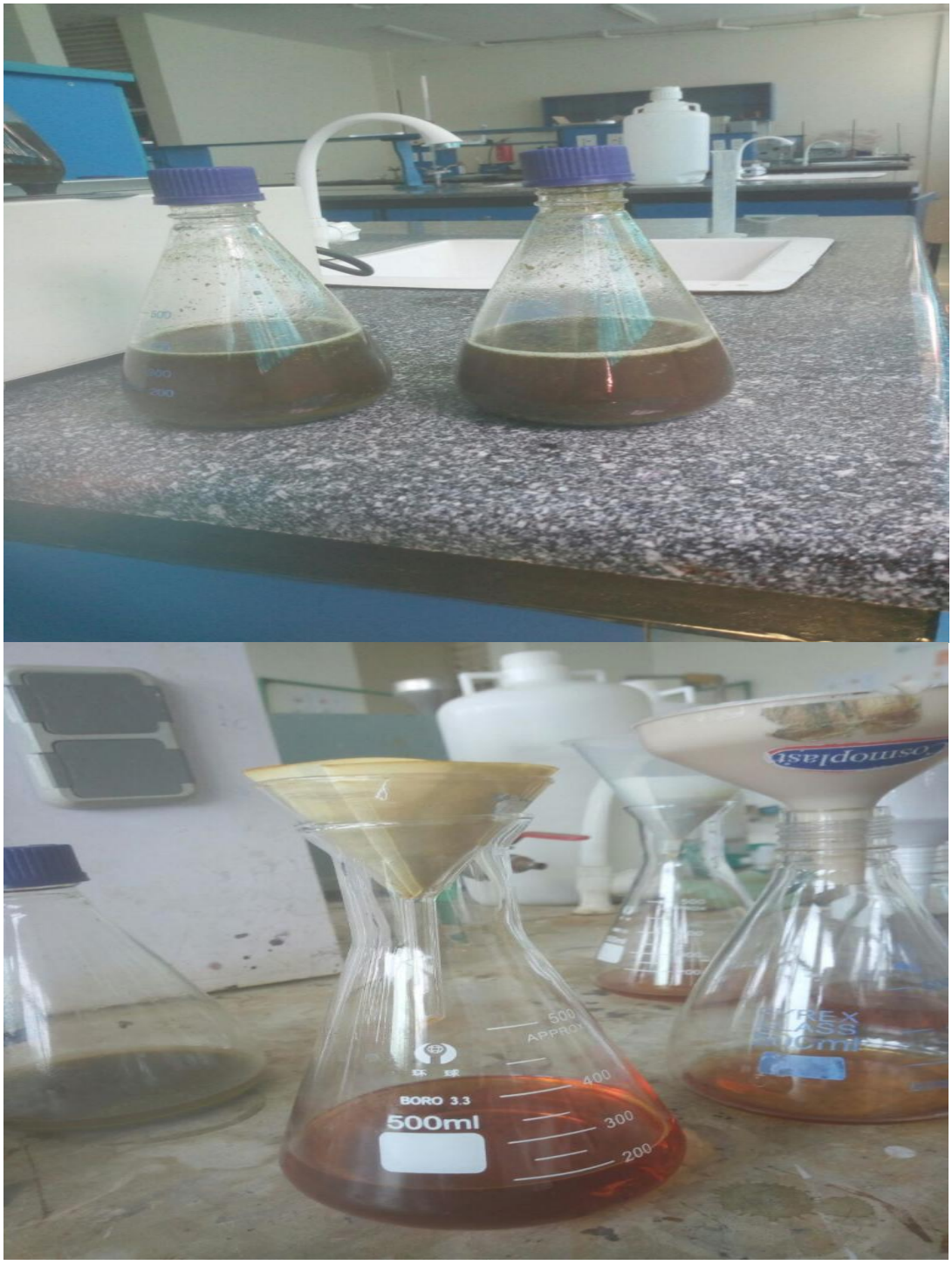

Figure 2: Plant leaf extract filtration

Figure 3: Synthesis of nanoparticles

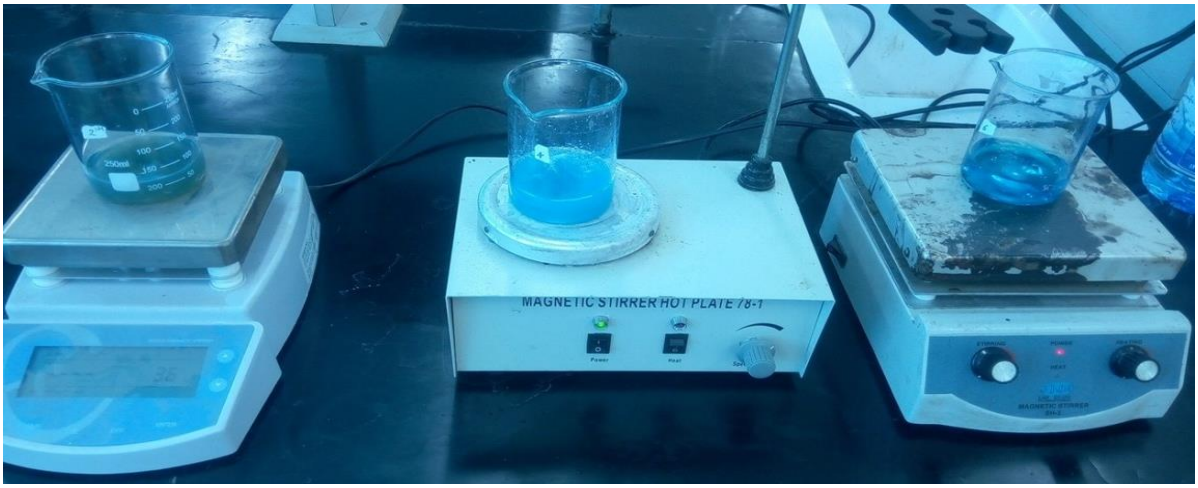

Figure 4: adsorption experiment stirring by digital magnetic stirrer using NPs

Figure 5: Filtration process in adsorption experiment

Figure 6: Working standard solution of methylene blue dye